NASA TN D-1478

N62-16104

TECHNICAL NOTE

D-1478

AN INVESTIGATION TO DETERMINE THE DISCHARGE AND THRUST CHARACTERISTICS OF AUXILIARY-AIR OUTLETS FOR A STREAM MACH NUMBER OF 3.25

By Allen R. Vick

Langley Research Center
Langley Station, Hampton, Va.

NATIONAL AERONAUTICS AND SPACE ADMINISTRATION

WASHINGTON

October 1962

NATIONAL AERONAUTICS AND SPACE ADMINISTRATION

TECHNICAL NOTE D-1478

AN INVESTIGATION TO DETERMINE THE DISCHARGE AND THRUST CHARACTERISTICS OF AUXILIARY-AIR OUTLETS FOR A STREAM MACH NUMBER OF 3.25

By Allen R. Vick

SUMMARY

An investigation to determine the discharge and thrust characteristics of a series of auxiliary-air outlets for a stream Mach number of 3.25 has been conducted. Thin-plate outlets with aspect ratio varying from 6 to 1/6 and ducted outlets with various shapes and angles of inclination with respect to the stream direction were tested. Ratios of outlet total pressure to free-stream static pressure ranged up to 44, and mass-flow ratios were as high as 4.

Results indicate that the sonic-flow coefficient reaches a maximum at pressure ratios on the order of 4 to 6 and is essentially independent of any further increases in pressure and/or mass-flow ratio. Average sonic-flow coefficients of about 0.87 were obtained for all thin-plate outlets and about 0.98 for all the ducted outlets. Results of thrust measurements indicate that thin-plate outlets may produce some thrust depending upon both aspect ratio and pressure ratio. The ducted outlets that discharged the air more nearly parallel to the free stream gave the highest thrust coefficients. Substantial increases in thrust coefficient were obtained by the use of various radii of curvature on the downstream side of the outlet. In general, the correlation of these data with those at subsonic and transonic Mach numbers appears to be such that reasonable estimations may be made of the discharge characteristics of auxiliary-air outlets at intermediate Mach numbers for the lower mass-flow ratios.

INTRODUCTION

The large volumes of secondary air which are used in supersonic aircraft require efficient handling if maximum vehicle performance is to be achieved. This air, used for cabin ventilation and equipment cooling, for boundary-layer control, for engine-inlet matching, and so forth, possesses considerable energy which can be converted to thrust if properly discharged from the aircraft.

Previous investigations of the discharge characteristics of flush thin-plate and inclined outlets (refs. 1 to 3) and of flapped outlets (ref. 4) have been presented for stream Mach numbers up to 1.30. Additional data on various flush and protruding configurations are found in references 5 to 8. The present experimental investigation, a continuation of those reported in references 1 to 4, was undertaken to extend the data on several of these outlets to a Mach number of 3.25. Thin-plate outlets of circular, rectangular, and elliptical cross section, ducted outlets whose axes were inclined at various angles to the stream flow, and a flapped outlet of aspect ratio 1.0 were investigated. Discharge characteristics and force data are presented as functions of outlet pressure ratio. The Reynolds number of the flow in the test section was approximately 3.52×10^6 per inch at an average total pressure of 310 lb/sq in. abs and a total temperature of 80° F.

SYMBOLS

A	aspect ratio
A_o	minimum outlet area, sq ft unless otherwise noted
C_T	thrust coefficient, T/qA_o
D	diameter
K_s	outlet sonic-flow coefficient, $\frac{\text{Measured mass flow}}{\text{Theoretical sonic mass flow}}$
M	Mach number
$\frac{p_{t,o}}{p_\infty}$	outlet pressure ratio; ratio of outlet total pressure to free-stream static pressure
q	free-stream dynamic pressure, $\frac{\rho V^2}{2}$, lb/sq ft
R	radius of curvature of inclined outlet, in.
T	thrust, lb
V	stream velocity, ft/sec
w	measured outlet mass flow, slugs/sec

$\frac{w}{w_o}$ discharge-flow ratio, $\frac{\text{Measured outlet mass flow}}{\text{Tunnel mass flow through area equal to outlet area}}$

β outlet-duct inclination relative to free stream, deg

δ_f flap angle, deg

η thrust efficiency, $\frac{C_{T,m}}{C_{T,i} \cos \beta}$

ρ tunnel air density, slugs/ft^3

Subscripts:

i ideal

m measured

APPARATUS AND PROCEDURE

Wind Tunnel

This investigation was conducted in the $9\frac{1}{2}$- by $9\frac{1}{2}$-inch test section of a fixed-geometry supersonic wind tunnel. A schematic diagram of the tunnel with air supply to the outlets is presented in figure 1. The Mach number determined from a total pressure in the settling chamber and a wall static pressure upstream of the outlet installation was 3.25. Air for the outlets, at a total pressure always less than that of the free-stream total pressure of 310 lb/sq in. abs, was supplied from the upstream settling chamber through a 2-inch pipe. The discharge flow through the outlet was controlled by a valve and measured by a calibrated metering nozzle.

Outlets

In this investigation three types of outlets were tested: flush thin plate (outlets 1 to 8), flush ducted (outlets 9 to 16), and ducted with an external flap protruding into the airstream (outlet 17). Schematic drawings of these outlets are shown in figures 2 and 3. The flush thin-plate outlets had circular, elliptical, and rectangular cross sections with aspect ratios from 6 to 1/6. The plate thickness for the

thin-plate models was 1/16 inch. Eight ducted outlets of circular and rectangular cross sections were inclined to the stream flow direction at angles varying from 90° to 30°. Three of the outlets inclined 60° were identical except for variations in the radius of curvature on the downstream side of the outlet. Figure 3(b) shows the outlet configuration with flap attached. The minimum outlet area A_o for the flapped configuration is somewhat ambiguous in that it neglects the area vented to the free stream on either end of the flap.

Pressure instrumentation consisted of transducers located close to the orifices in order to minimize time lag; their output was continuously recorded on self-balancing potentiometers. A screen was located upstream of the metering nozzle (fig. 1) to improve the flow uniformity. Outlet total pressure was measured in the supply line just upstream of the outlet as shown in figure 4.

Thrust Balance

The thrust-balance and outlet-support arrangement was of the floating-body type and is shown in figure 4. This arrangement consists primarily of a floating model holder connected by four flexible beams to a rigid support structure. Outlet air is supplied to the floating body through a piece of tubing bearing only on "O" ring seals at each end. Axial force produced by the outlet discharge caused a movement of the floating body which applied a load to an unbonded strain gage. The strain gage, with a full-load deflection of ±0.0015 inch, was connected to a recording potentiometer. A gap of 0.005 inch existed between the floating part and the tunnel wall, and a fouling light was used to indicate any contact. In order to minimize flow through the gap, the thrust balance was surrounded by an airtight enclosure which maintained the pressure surrounding the balance within 1 lb/sq in. of the tunnel static pressure. Tare forces produced as a result of this pressure differential, the outlet-supply-line pressure, and the friction force on the flat plate mounted in the model holder necessitated small corrections in the force data. All thrust data were recorded continuously on an automatic data plotter.

DISCUSSION OF RESULTS

Discharge Characteristics

The outlets of this investigation fall into three categories: flush thin plate, flush ducted, and ducted with an external flap projecting into the airstream. Typical data plots of four representative outlets

are presented in figure 5. Included in this figure are data for the four representative outlets: two thin-plate outlets (2 and 8) which cover the maximum spread of the test results for this type of outlet, one flush ducted outlet (15), and the flapped outlet (17). The data of figure 5(a) are presented in the form of a sonic-flow coefficient K_s plotted against the outlet-pressure ratio. The sonic-flow coefficient for each of the outlets increases rapidly with pressure ratio, reaching an average of 90 to 95 percent of its maximum value at pressure ratios of approximately 3. The maximum value attained at pressure ratios on the order of 6 was essentially independent of any further increases in pressure ratio. Whereas maximum values of K_s for the flush outlets approached unity, that of the flapped outlet exceeded 1.0 as a result of differences between the effective throat area and the throat area as defined in the calculations.

Discharge-flow ratio presented as a function of outlet-pressure ratio for the four representative outlets (2, 8, 15, and 17) is shown in figure 5(b). This discharge-flow ratio is the ratio of the outlet mass flow to the tunnel mass flow through a stream tube having an area equal to that of the outlet. Above pressure ratios of about 3, the variation of discharge-flow ratio is essentially linear. The differences in the discharge coefficients (fig. 5(a)) are reflected in figure 5(b) by the slopes of the lines; that is, the lines for the thin-plate outlets had the lowest slopes, and the highest slope was obtained with the flapped outlet. The discharge characteristics of these outlets are divided roughly into three groups: thin plate, ducted, and flapped. A summary of these data including those previously discussed is presented in figure 6. Data points are omitted in this figure and in most cases no effort is made to distinguish between individual outlets of a given type.

The sonic-flow coefficient for all eight ducted outlets (outlets 9 to 16; fig. 6(a)) increases rapidly with increasing pressure ratio; maximum values are obtained at pressure ratios as low as 3 to 4 in some cases. Average flow coefficients of about 0.98 are attained at pressure ratios on the order of 6. At higher pressure ratios, the flow coefficient is independent of the duct cross section or angle of inclination.

The sonic-flow coefficient for thin-plate and flapped outlets (outlets 1 to 8 and outlet 17, respectively; fig. 6(b)) shows the same general characteristics as for the ducted outlets. An average value of K_s on the order of 0.87 is obtained for six of the thin-plate outlets and is again independent of shape or of pressure ratios higher than approximately 6. The two thin-plate outlets of aspect ratio 6 (outlet 7) and 1/6 (outlet 8) give slightly higher sonic-flow coefficients and the maximum value is reached at a lower pressure ratio. Flapped-outlet data are generally similar to the data for the thin plate and ducted outlets. Figure 6(c) is a summary plot of the variation of discharge-flow ratio with pressure ratio for all outlets tested.

Low-Pressure-Ratio Operation

A more detailed study of the discharge characteristics at low-pressure-ratio operation is presented in figures 7, 8, and 9 for thin-plate, ducted, and flapped outlets, respectively. For each outlet, sonic-flow coefficient is plotted against pressure ratio and discharge-flow ratio. Also presented for comparison are data at other Mach numbers obtained from references 1 to 4. These data show a generally substantial Mach number effect existing at low pressure ratios. As Mach number increases a higher pressure ratio is required to maintain a given discharge-flow coefficient; exceptions to this trend are noted in figures 7(g) and (h) for the thin-plate outlets with aspect ratios of 6 and 1/6. At a constant low discharge-flow ratio, the sonic-flow coefficient increases quite rapidly with increasing Mach number. As the discharge-flow ratio increases and approaches 1.0, the Mach number effect on the flow coefficient tends to disappear.

Data for the ducted and flapped outlets (figs. 8 and 9) exhibit qualities similar to the thin-plate data. In all instances, the maximum value of sonic-flow coefficient is obtained at relatively low discharge-flow ratios and remains essentially constant for further increases in flow rate.

A sample cross plot of the data from figure 7(b) is shown in figure 10 as the variation of discharge-flow ratio with pressure ratio for different Mach numbers. As Mach number increases from 0.7 to 3.25 there is a substantial decrease in the slope of the curves which indicates that a much higher pressure ratio is required to maintain a constant discharge-flow ratio. This requirement is shown more clearly by the cross plot in figure 11 at constant values of mass-flow ratio. The correlation of these data with those at subsonic and transonic Mach numbers appears to be such that reliable estimations may be made of the discharge characteristics of auxiliary-air outlets in the intervening Mach number range.

No-Flow Pressures

Pressure characteristics of outlets, in which no air is being discharged, are often of interest to aircraft designers from the standpoint of resultant pressures produced by certain openings or holes in the aircraft skin. These pressure ratios can be read from figures 7 to 9 for a sonic-flow coefficient of zero. As the speed increased beyond transonic values, no-flow pressures much higher than ambient pressures were measured below the opening. Reference 9 indicates that the pressure buildup is related to an inflow of air at the downstream end of the opening with a subsequent vortex formation within the outlet. A comprehensive investigation of flow in a cavity (ref. 10) shows in all

cases a much higher pressure on the downstream face of the outlet as a result of shock formations just ahead of the downstream lip. Shocks occur only when air attempts to flow into and then out of the opening.

In figure 12 pressure ratio is plotted against aspect ratio for thin-plate outlets; this cross plot reveals that the maximum pressure ratio is a function of aspect ratio. The range of aspect ratio between 2 and 3 produces maximum no-flow pressure ratio. Similar results are noted for transonic data with peak no-flow pressures occurring at higher aspect ratio. The sharp decrease in pressure at an aspect ratio of 1/6 is similar to the results of reference 10 which showed the cavity pressure distribution to be very sensitive to changes in aspect ratio less than 0.25. The effects of Mach number on no-flow pressure ratio are shown in figure 13 at constant values of aspect ratio. For a given outlet the no-flow pressure ratio increases sharply above transonic Mach numbers. Maximum pressure ratios are obtained over the entire Mach number range for aspect ratios of 2 and 3. (See fig. 13.)

Ducted outlets also show a considerable range of pressure variations as the angle of duct inclination is varied. (See fig. 14.) At angles of inclination above 60° the pressure is essentially independent of duct inclination. As the angle of inclination approaches a discharge direction more nearly parallel with the free stream, a trend is established for decreasing pressures.

Thrust Performance

Thrust-performance curves for all outlets are summarized in figure 15. Data are presented as the variation of thrust coefficient C_T with pressure ratio, where the thrust coefficient is defined as the ratio of measured thrust to the product of free-stream dynamic pressure and outlet area. For comparison purposes, an ideal thrust coefficient is also shown. This ideal thrust coefficient is based on the thrust calculated by the sum of the momentum and pressure-area relationships for a sonic nozzle alined with the free stream at various pressure ratios. Significant values of thrust are produced only by the inclined ducted outlets. The highest thrust coefficients for ducted outlets without flaps were for outlets 11 and 15 for which the angle of inclination relative to the free stream was least ($\beta = 30°$). No change in thrust coefficient was produced when the outlet-duct cross section was changed from circular (outlet 11) to square (outlet 15) and when the angle of inclination remained constant.

The incorporation of a radius of curvature on the downstream side of the outlet increased significantly the thrust coefficient as shown by the curves for outlets 12, 13, and 14 ($\beta = 60°$). Increasing the

radius of curvature increases the thrust coefficient about 95 percent at a pressure ratio of 6 and about 42 percent at a pressure ratio of 34. The ducted outlet 17 with the external flap produced the maximum thrust coefficient obtained in these tests. However, as previously stated, the effective area includes some area on both ends of the flap and is considerably larger than the area used in computation. Since the area appears in the denominator of the thrust-coefficient equation $\left(C_T = \frac{T}{qA_o}\right)$, the thrust coefficient should be correspondingly lower.

A more effective method of outlet comparison is shown in figure 16, which shows the relative thrust efficiency of the various ducted and flapped outlets in the form of outlet-thrust efficiency plotted against pressure ratio. Thrust efficiency is defined as the ratio of measured thrust coefficient $C_{T,m}$ to an ideal thrust coefficient $C_{T,i}$, which is based upon the streamwise component for a sonic nozzle discharging air at different angles relative to the stream flow direction. Comparisons of different angles of inclination reveals that as β is decreased from 60° to 30°, a more pronounced improvement in efficiency occurs at the low pressure ratios. As pressure ratio increases, the slope of the curve appears to be flattening out at a much more rapid rate for $\beta = 30°$ than for $\beta = 60°$. Further increases in thrust efficiency are apparent for the curved and flapped outlets. As previously pointed out, the measured thrust coefficient for the flapped outlet is probably high because of a larger effective area than the value used in computations. The ideal thrust coefficient for the flapped outlet assumes the discharge direction to be equal to the flap angle.

The improvement in thrust efficiency associated with increasing radius of curvature on the downstream end of the outlet inclined 60° was such that maximum efficiencies of about 85 percent were achieved at the highest pressure ratios; these efficiencies exceeded the results of all other outlets tested in this investigation. (See fig. 16(b).)

The data shown in figure 15 for the thin-plate and perpendicularly ducted outlets have been reproduced in an expanded scale in figure 17. It is important to note from this figure that, depending on the available pressure ratio, thrust may be obtained with either the perpendicularly ducted or thin-plate outlets. Similar results have been observed in unpublished transonic data and also noted in references 7 and 11. While the magnitude of thrust produced may be of only academic interest, a comparison of results in figures 17(a) and (b) reveals that a thin-plate outlet of aspect ratio 1.0 produces several times more thrust than a ducted outlet of comparable aspect ratio when discharging air normal to the stream direction.

A cross plot of C_T and aspect ratio for thin-plate outlets at constant values of pressure ratio (fig. 18) indicates that there is an optimum aspect ratio for best performance of thin-plate outlets. In general, a selection of aspect ratio varying from 2 to 4 results in highest thrust performance for thin-plate outlets. The maximum pressure ratio available for discharging air has no apparent effect on selection of aspect ratio.

The variation of thrust coefficient with Mach number for two of the ducted outlets is shown in figure 19 at constant values of discharge-flow ratio. Regardless of the large Mach number span between data of reference 3 and the present tests, curves connecting the data points were drawn with no abrupt deviations. The fairing of these curves indicates that reliable estimations of thrust coefficient are possible in the Mach number range from 0.4 to 3.25. Similar results for the flapped outlet along with subsonic and transonic data from reference 4 are shown in figure 20. The transonic drag rise at no flow is as severe as expected with a subsequent large variation in thrust coefficient over the Mach number range. The thrust coefficient at $M = 3.25$ generally exceeds lower Mach number values for discharge-flow ratios up to about 0.5; at higher discharge-flow ratios the trend is reversed.

No-flow thrust coefficient as a function of angle of inclination for the ducted outlets and as a function of aspect ratio for the thin-plate outlets is given in figure 21. In general, angle of inclination for the ducted outlets has very little effect on the no-flow thrust coefficient. (See fig. 21(a).)

SUMMARY OF RESULTS

An investigation of the discharge and thrust characteristics of auxiliary-air outlets for a stream Mach number of 3.25 indicates the following results:

1. Average sonic-flow coefficients of about 0.87 and 0.98 were obtained at pressure ratios greater than 4 to 6 for thin-plate and ducted outlets, respectively.

2. The discharge characteristics obtained in these tests correlated readily with those obtained for similar configurations at subsonic and transonic Mach numbers.

3. No-flow pressure characteristics of thin-plate outlets were strongly dependent upon aspect ratio.

4. Significant amounts of thrust, depending upon the angle of inclination and the pressure ratio, were achieved for ducted outlets. Incorporation of various radii of curvature on the downstream side of an outlet inclined 60° produced greater increases in thrust efficiency than an outlet inclined 30°. Maximum thrust efficiencies of about 85 percent were achieved at the highest pressure ratios with the ducted outlets.

5. Thin-plate outlets produced finite values of thrust, depending upon both aspect ratio and pressure ratio.

Langley Research Center,
National Aeronautics and Space Administration,
Langley Station, Hampton, Va., July 9, 1962.

REFERENCES

1. Nelson, William J., and Dewey, Paul E.: A Transonic Investigation of the Aerodynamic Characteristics of Plate- and Bell-Type Outlets for Auxiliary Air. NACA RM L52H20, 1952.

2. Dewey, Paul E.: A Preliminary Investigation of Aerodynamic Characteristics of Small Inclined Air Outlets at Transonic Mach Numbers. NACA TN 3442, 1955. (Supersedes NACA RM L53C10.)

3. Dewey, Paul E., and Vick, Allen R.: An Investigation of the Discharge and Drag Characteristics of Auxiliary-Air Outlets Discharging Into a Transonic Stream. NACA TN 3466, 1955.

4. Vick, Allen R.: An Investigation of Discharge and Thrust Characteristics of Flapped Outlets for Stream Mach Numbers From 0.40 to 1.30. NACA TN 4007, 1957.

5. Anderson, D. C.: Efficiency of Flush and Protruding Oblique Exhaust Nozzles With and Without External Flow. Rep. R-0955-22, United Aircraft Corp. Res. Dept., Oct. 1957.

6. Abdalla, Kaleel L.: Performance Characteristics of Flush and Shielded Auxiliary Exits at Mach Numbers of 1.5 to 2.0. NASA MEMO 5-18-59E, 1959.

7. McLafferty, G. H., Krasnoff, E. L., Ranard, E. D., Rose, W. G., and Vergara, R. D.: Investigation of Turbojet Inlet Design Parameters. Rep. R-0790-13, United Aircraft Corp. Res. Dept., Dec. 1955.

8. Crossen, J. W.: Efficiency of Flush Oblique Nozzles Exhausting Into Supersonic Streams Having Mach Numbers up to 4. Rep. R-1285-10, United Aircraft Corp. Res. Dept., Sept. 1959.

9. Roshko, Anatol: Some Measurements of Flow in a Rectangular Cutout. NACA TN 3488, 1955.

10. McDearmon, Russel W.: Investigation of the Flow in a Rectangular Cavity in a Flat Plate at a Mach Number of 3.55. NASA TN D-523, 1960.

11. Rogallo, F. M.: Internal-Flow Systems for Aircraft. NACA Rep. 713, 1941.

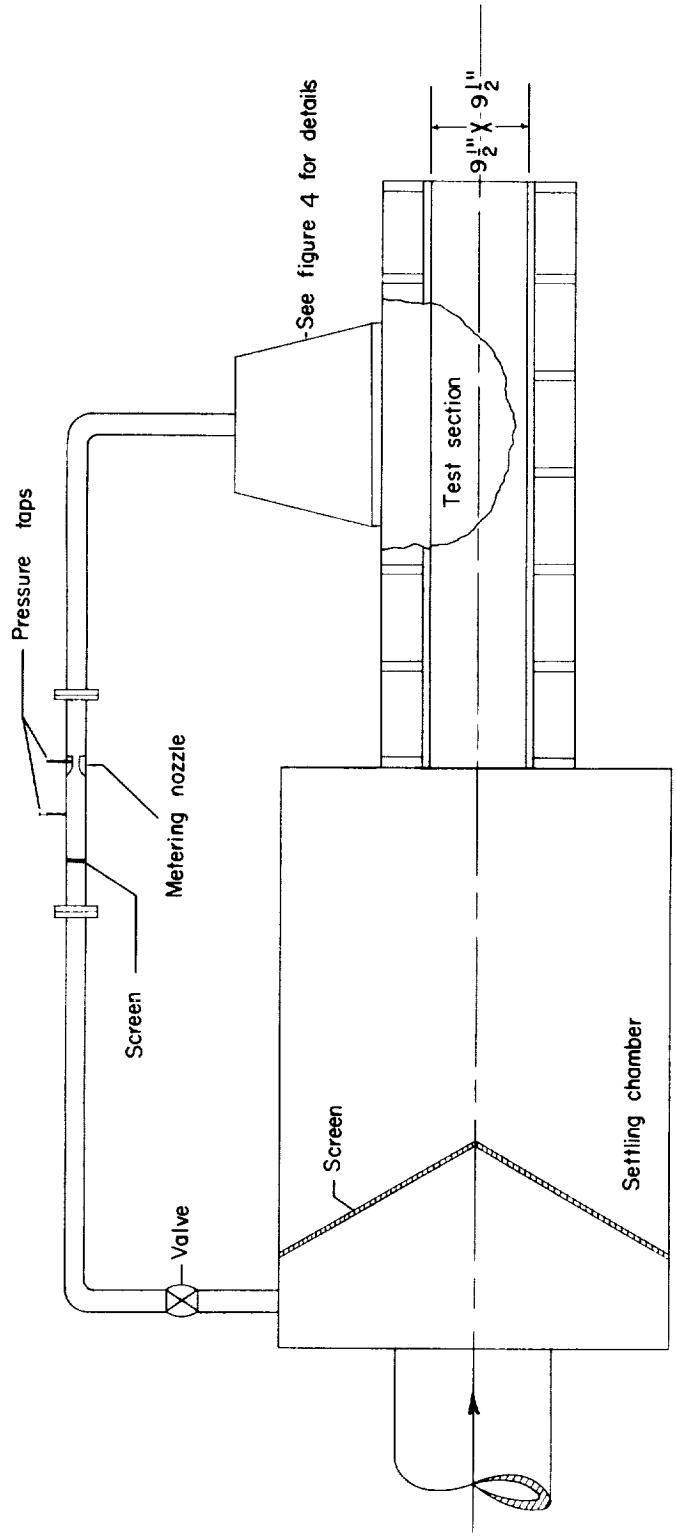

Figure 1.- Schematic diagram of tunnel with air supply to outlets.

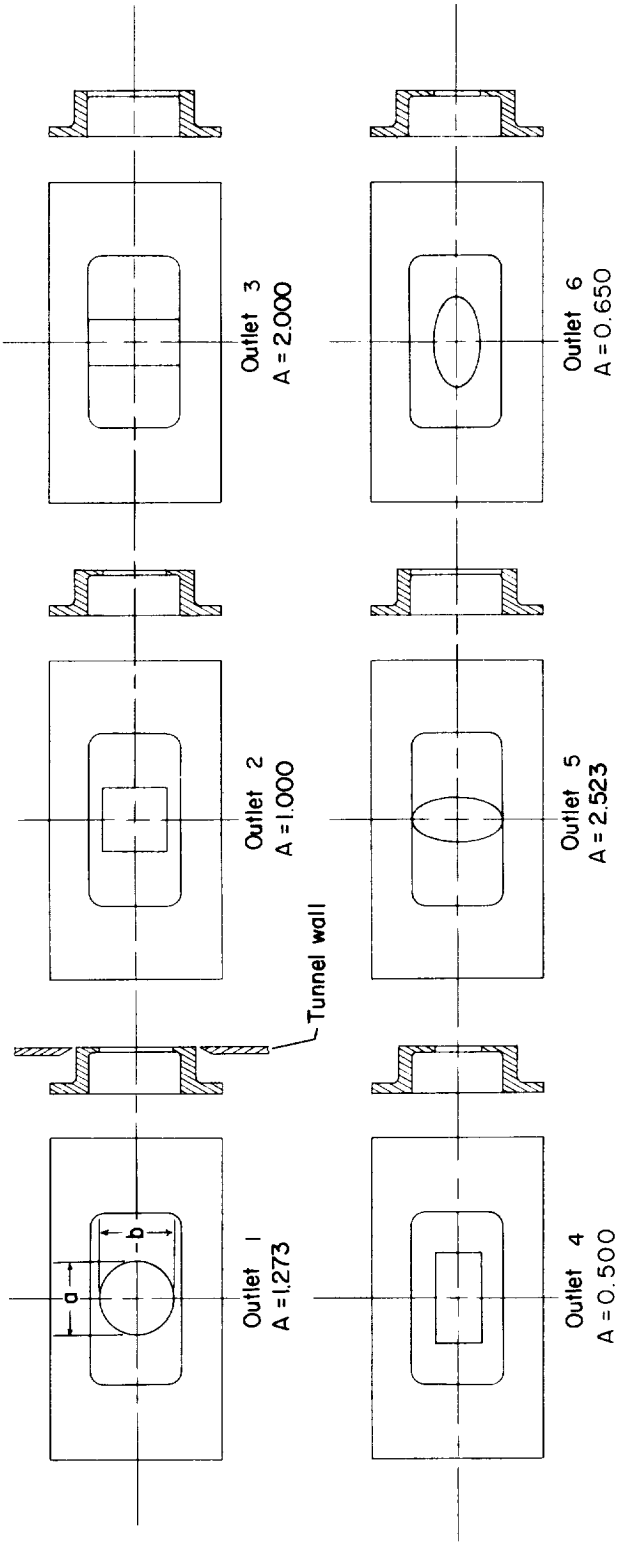

Outlet	Dimensions a, in.	b, in.	Area, sq in.
1	0.796	0.796	0.4976
2	.707	.709	.5013
3	.501	1.006	.5040
4	.996	.504	.5020
5	.504	.999	.3954
6	.993	.507	.3954
7	.165	.997	.1645
8	.997	.165	.1645

Figure 2.- Schematic diagrams and table of dimensions and areas for flush thin-plate outlets. Plate thickness = 1/16 in. Tunnel-air flow direction from left to right.

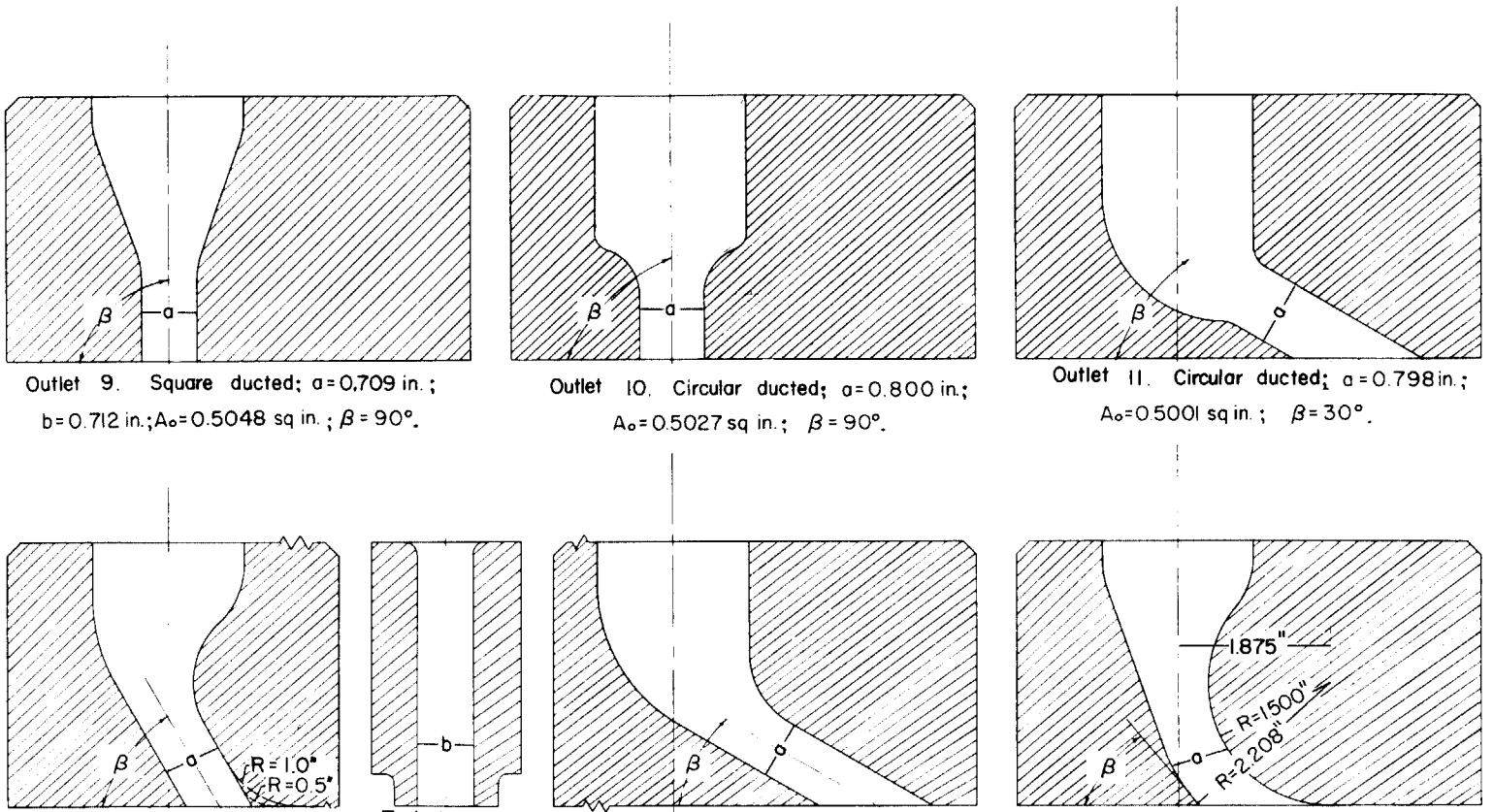

(a) Schematic diagrams and dimensions of ducted outlets.

Figure 3.- Cross-section view of ducted outlets.

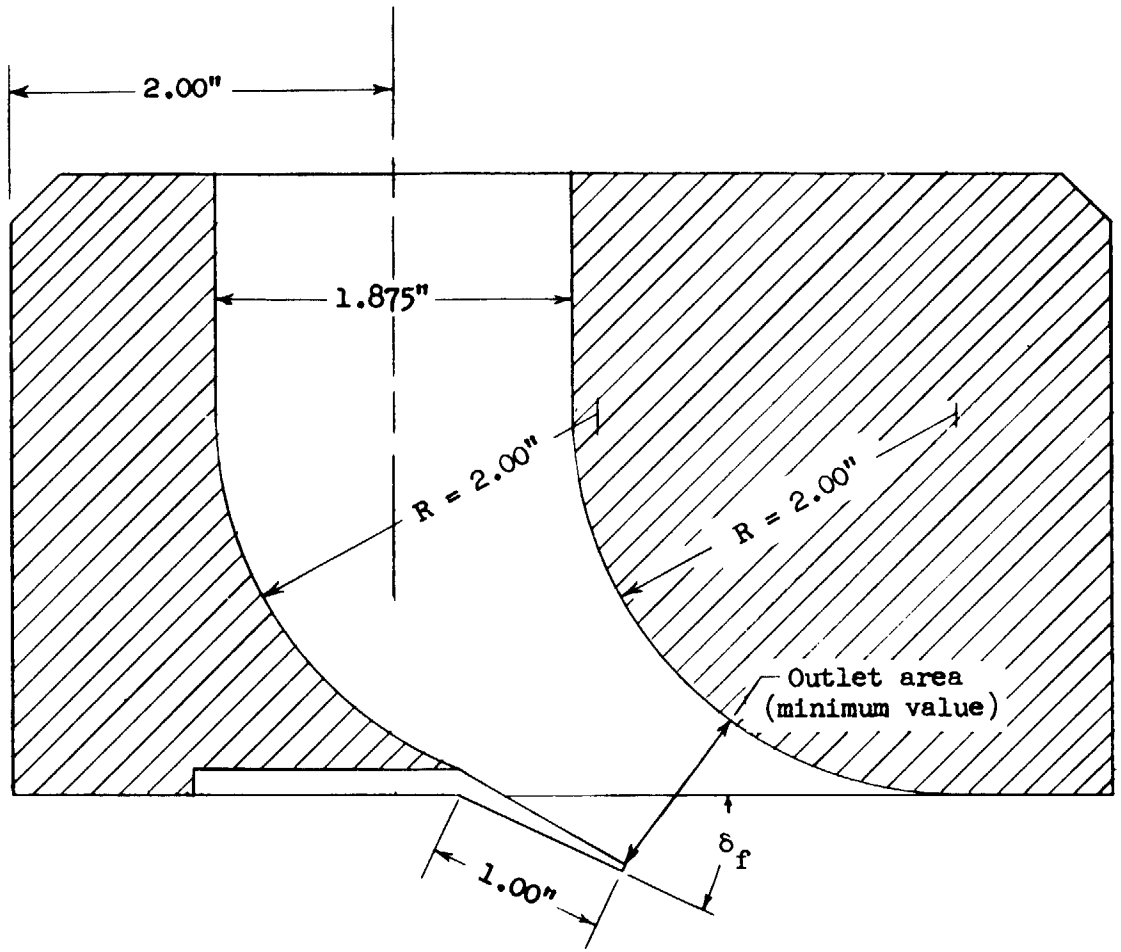

(b) Schematic diagram of ducted configuration with flap installed. Outlet 17; A_o = 0.8825 sq in.; $\delta_f = 25°21'$.

Figure 3.- Concluded.

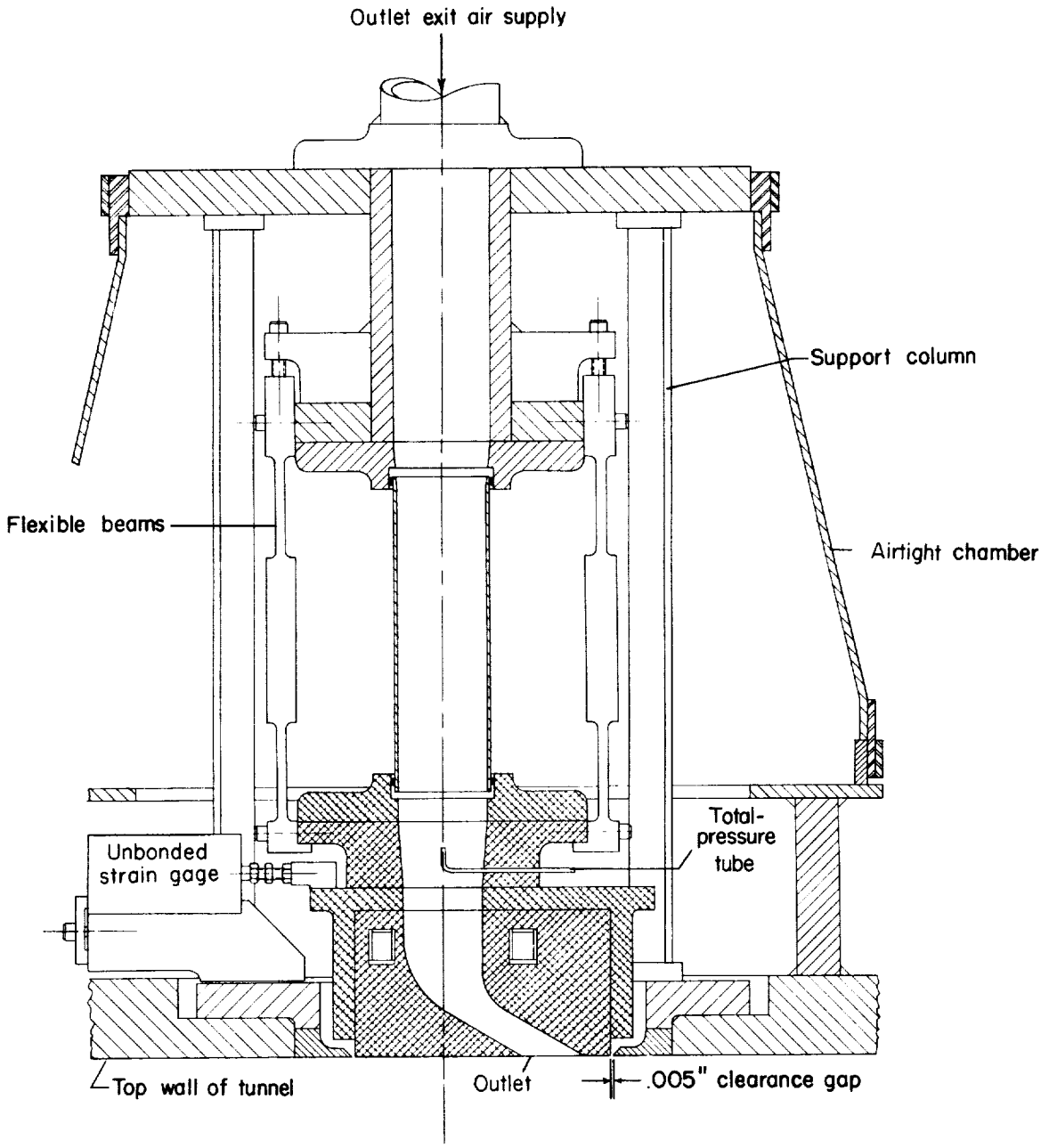

Figure 4.- Schematic diagram of thrust-balance and outlet installation.

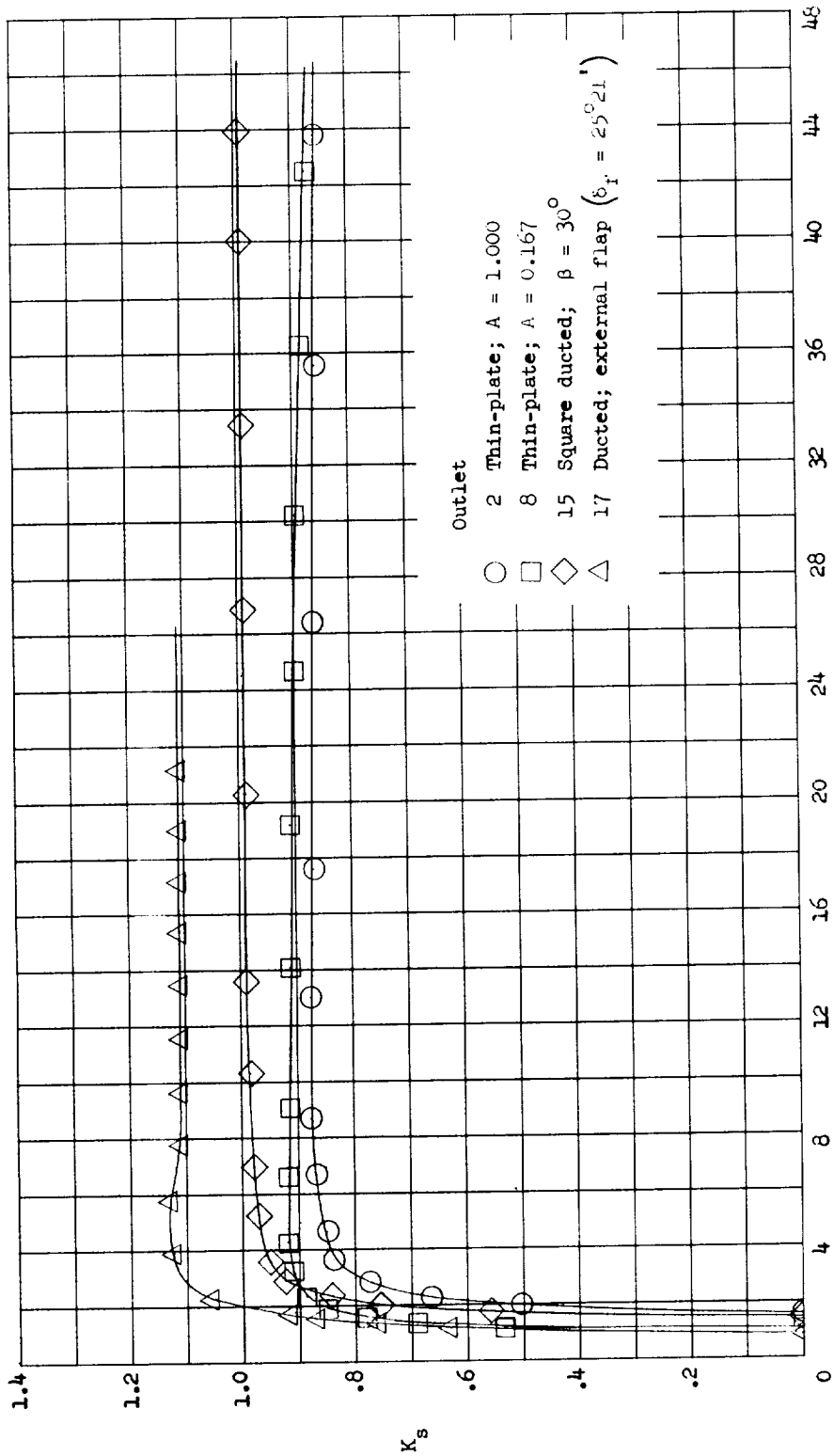

(a) Variation of sonic-flow coefficient with pressure ratio.

Figure 5.- Data plots for four representative outlets.

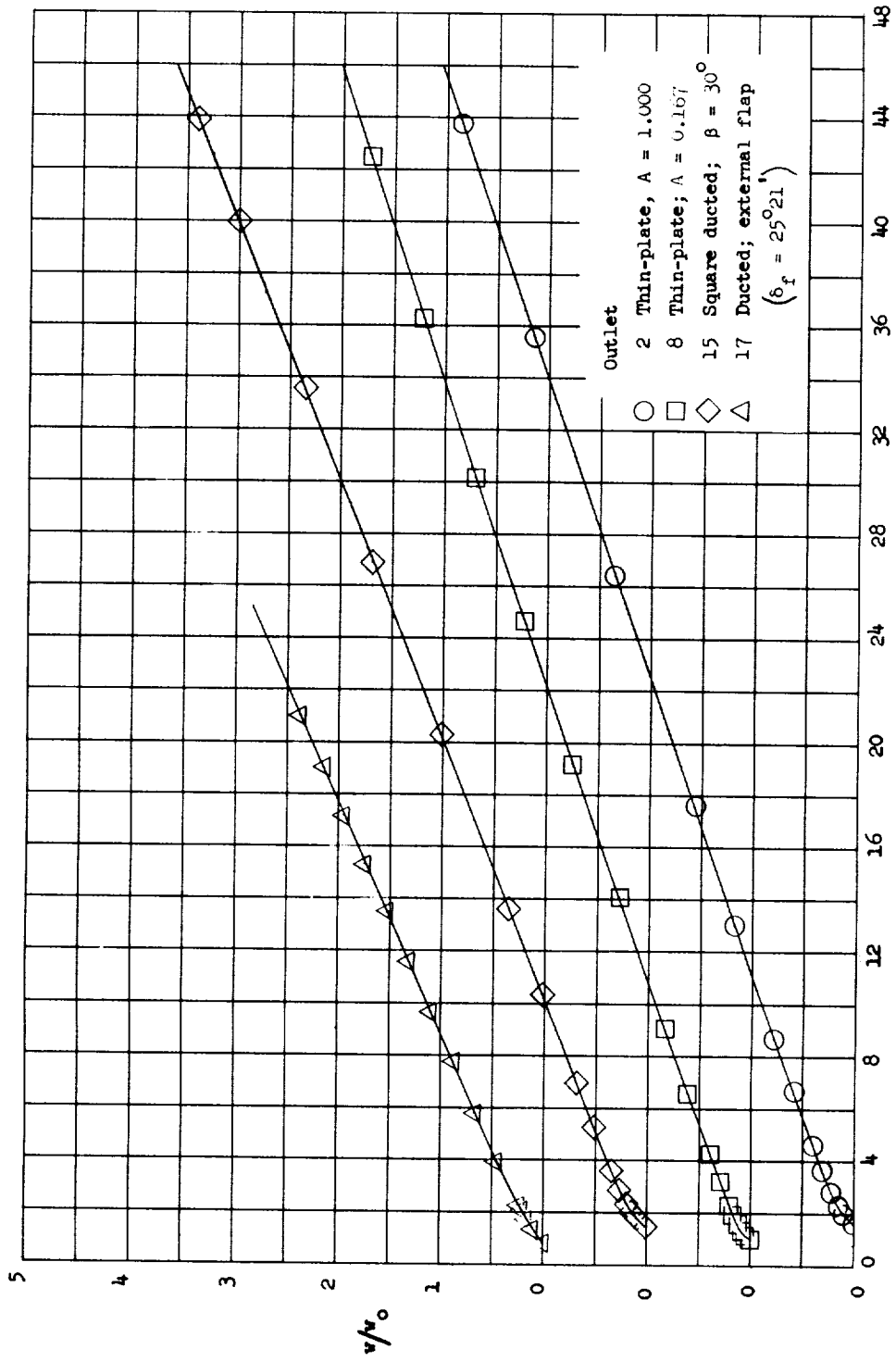

(b) Variation of discharge-flow ratio with pressure ratio.

Figure 5.- Concluded.

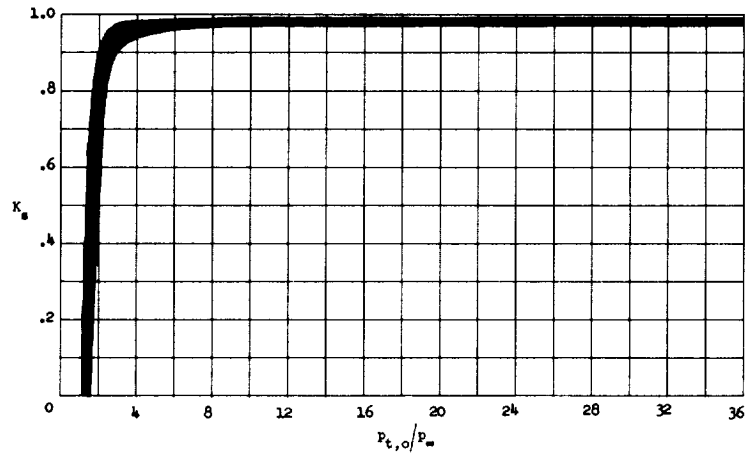

(a) Variation of sonic-flow coefficient with pressure ratio for all eight ducted outlets (9 to 16).

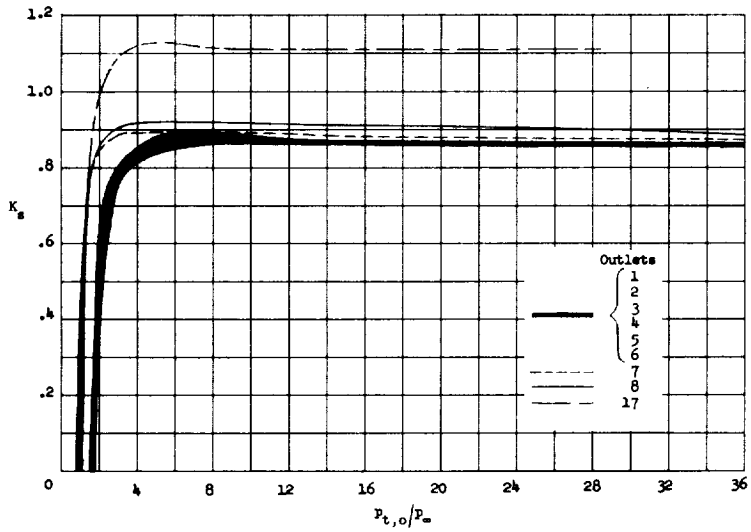

(b) Variation of sonic-flow coefficient with pressure ratio for all eight flat-plate outlets and for the flapped outlet.

Figure 6.- Summary of flow characteristics for all outlets.

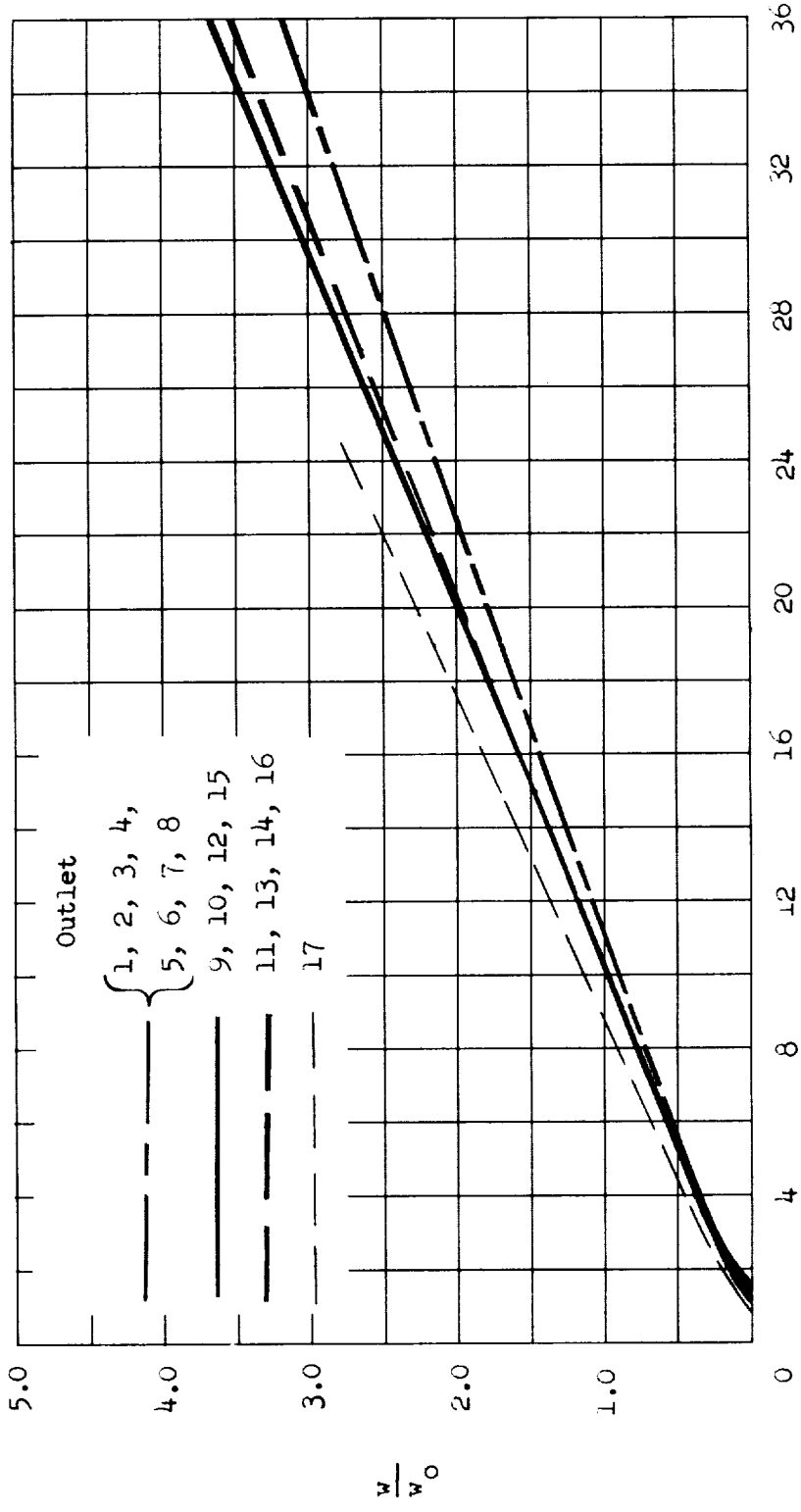

(c) Variation of discharge-flow ratio with pressure ratio for all outlets tested.

Figure 6.- Concluded.

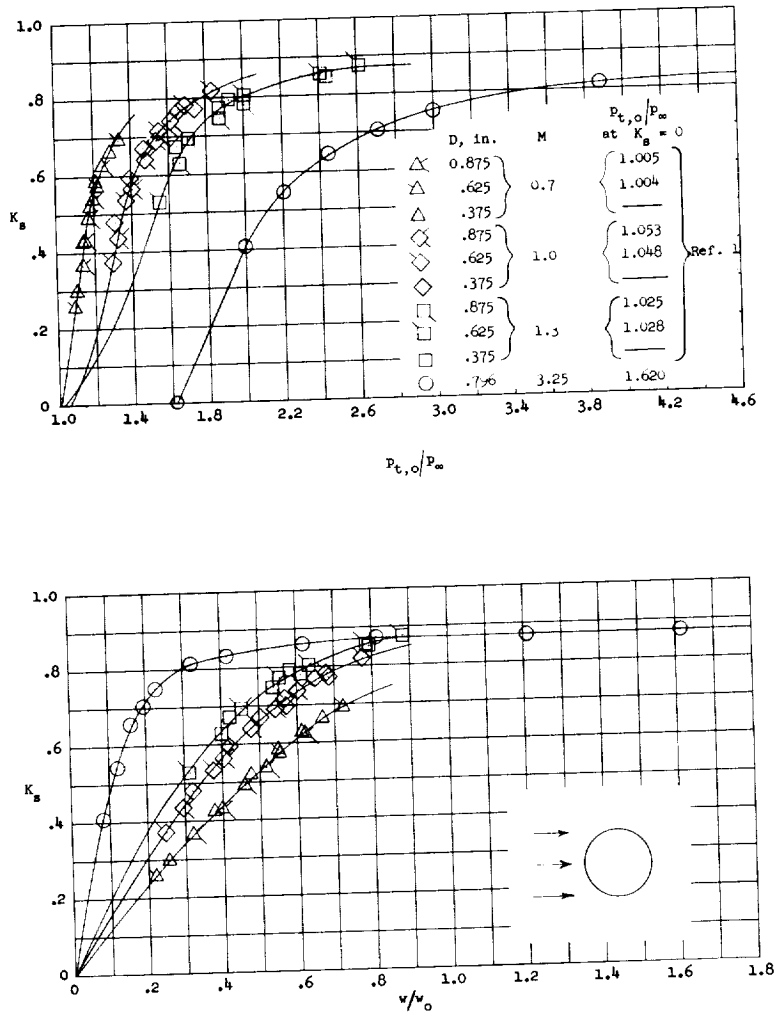

(a) Circular thin-plate outlet 1. A = 1.273.

Figure 7.- Discharge characteristics of thin-plate outlets.

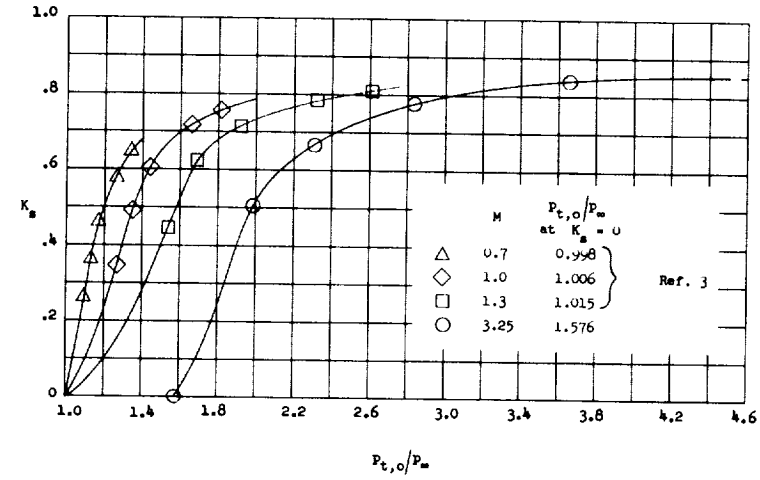

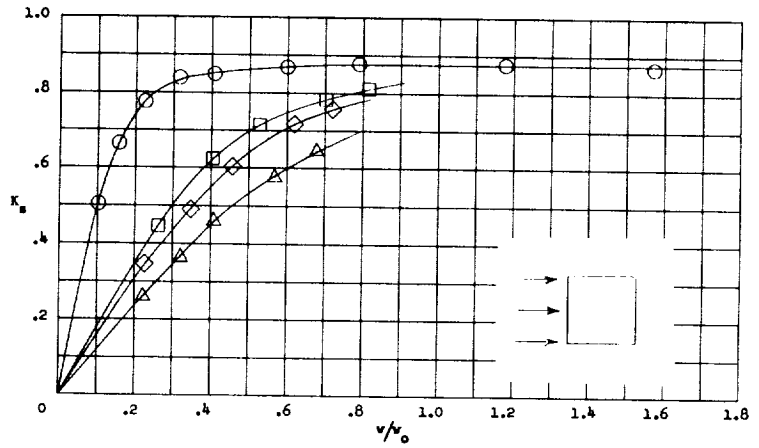

(b) Square thin-plate outlet 2. A = 1.0.

Figure 7.- Continued.

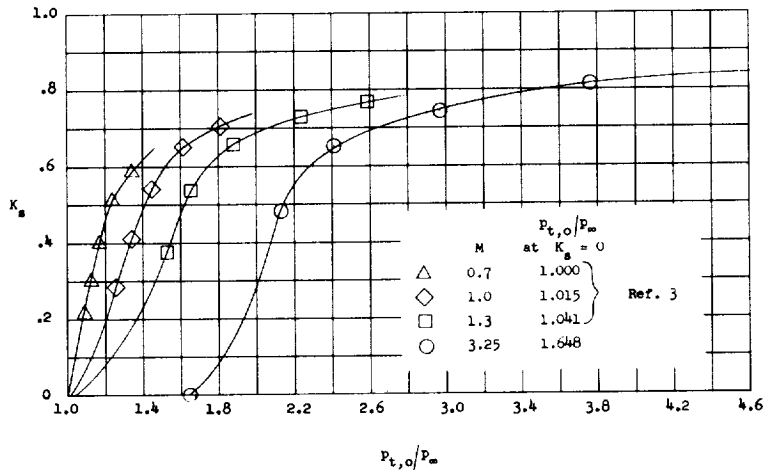

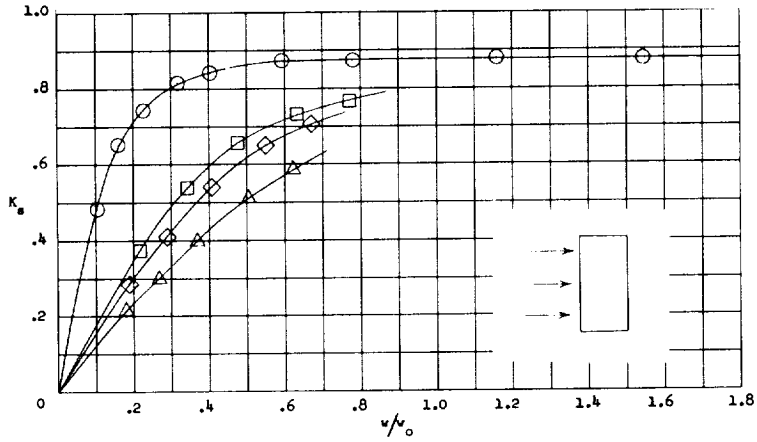

(c) Rectangular thin-plate outlet 3. A = 2.0.

Figure 7.- Continued.

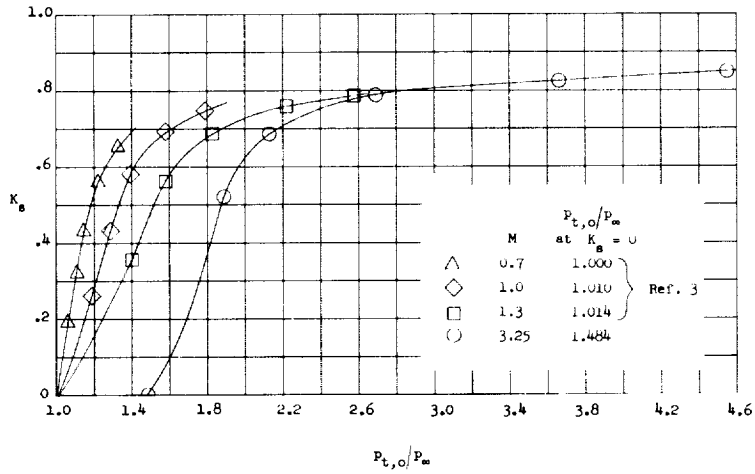

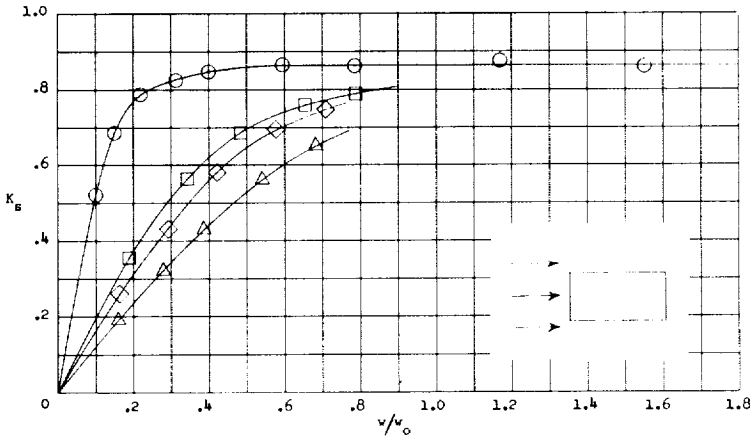

(d) Rectangular thin-plate outlet 4. A = 0.5.

Figure 7.- Continued.

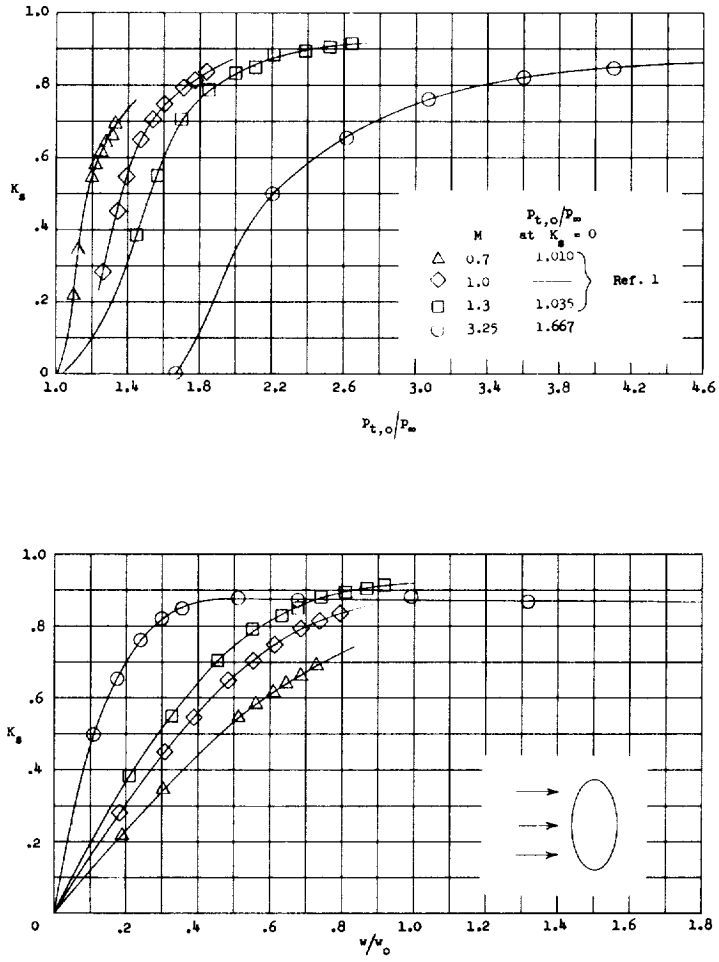

(e) Elliptical thin-plate outlet 5 with major- to minor-axis ratio of 2 to 1 (major axis perpendicular to airflow). A = 2.523.

Figure 7.- Continued.

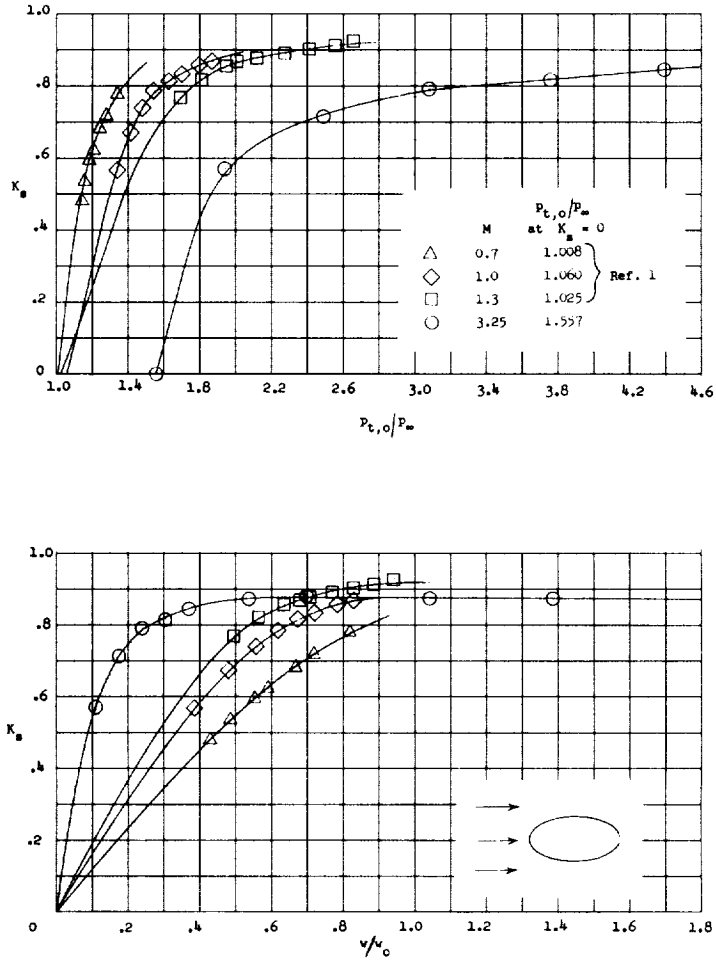

(f) Elliptical thin-plate outlet 6 with major- to minor-axis ratio of 2 to 1 (major axis parallel to airflow). A = 0.650.

Figure 7.- Continued.

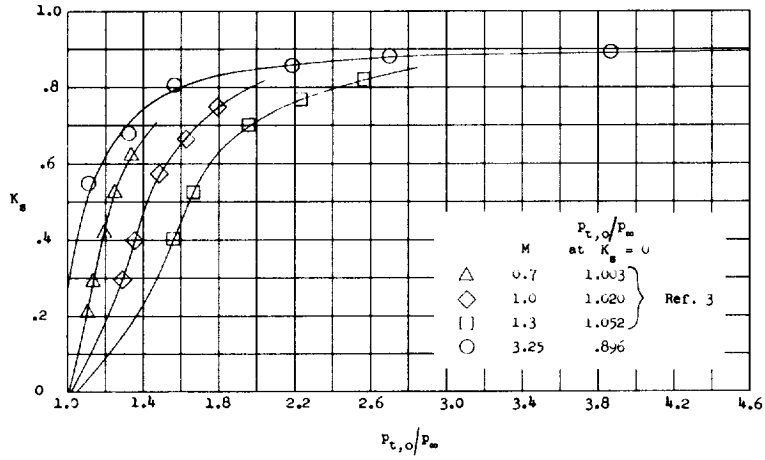

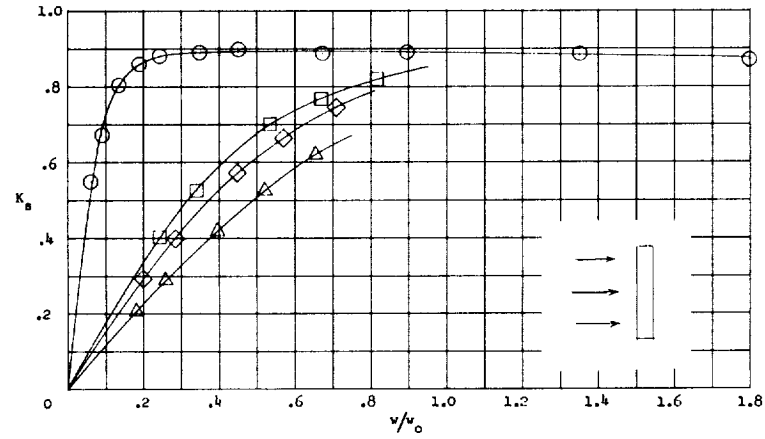

(g) Rectangular thin-plate outlet 7. A = 6.0.

Figure 7.- Continued.

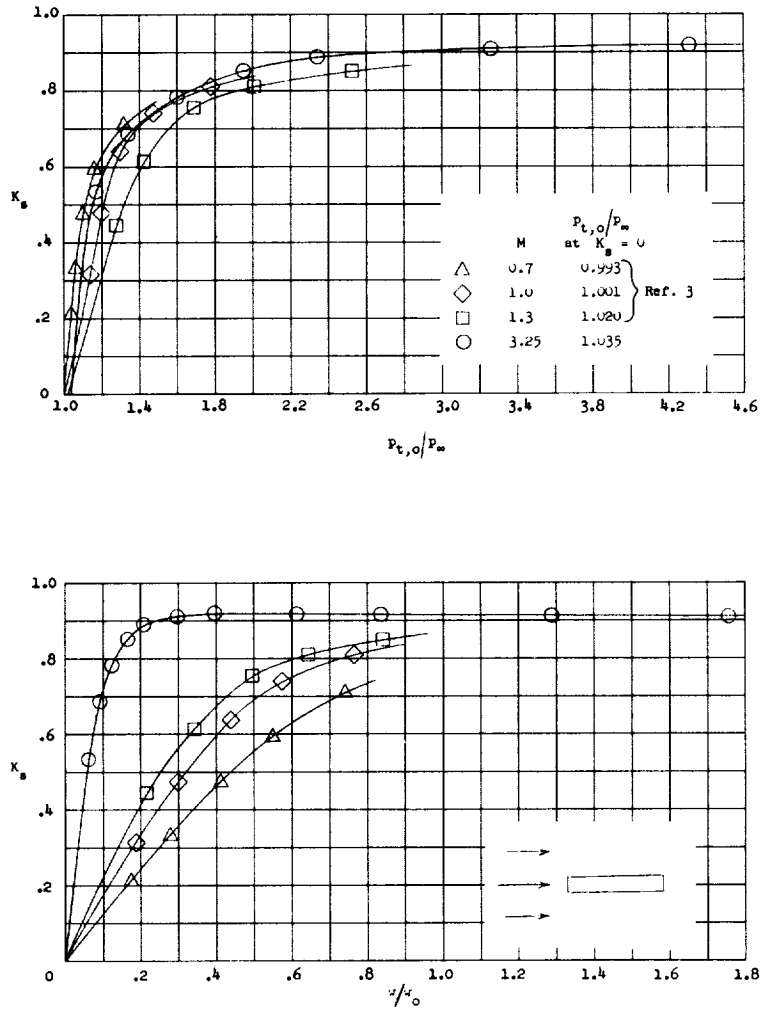

(h) Rectangular thin-plate outlet 8. A = 1/6.

Figure 7.- Concluded.

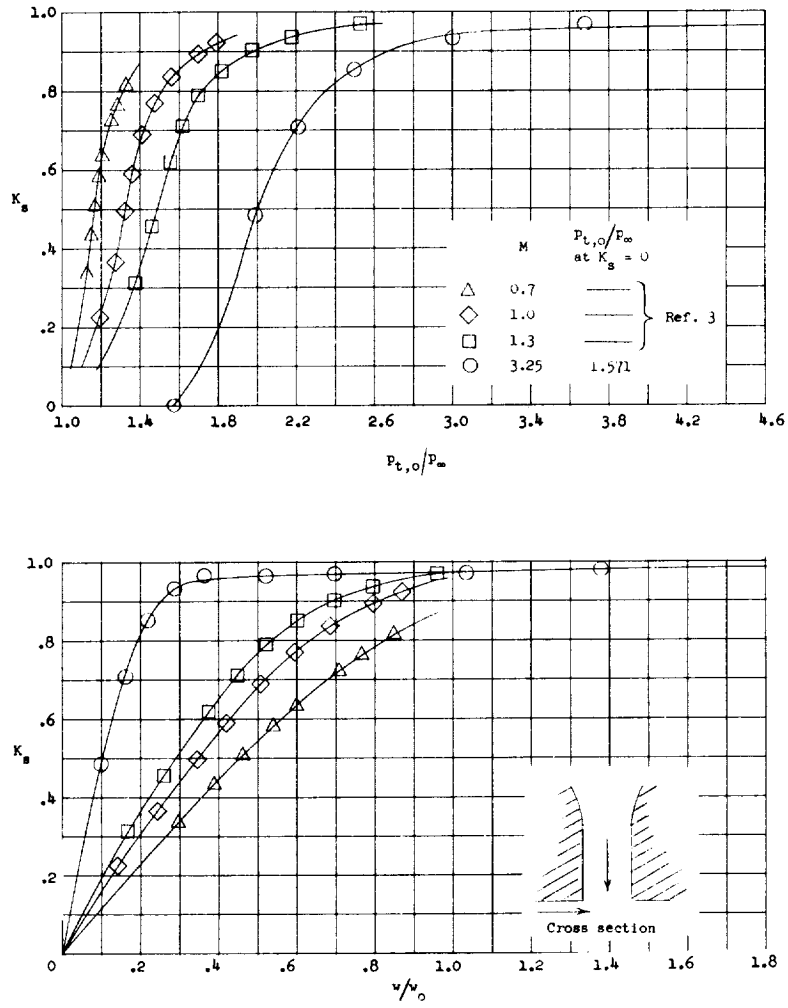

(a) Square ducted outlet 9. A = 1.0; $\beta = 90^\circ$.

Figure 8.- Discharge characteristics of ducted outlets.

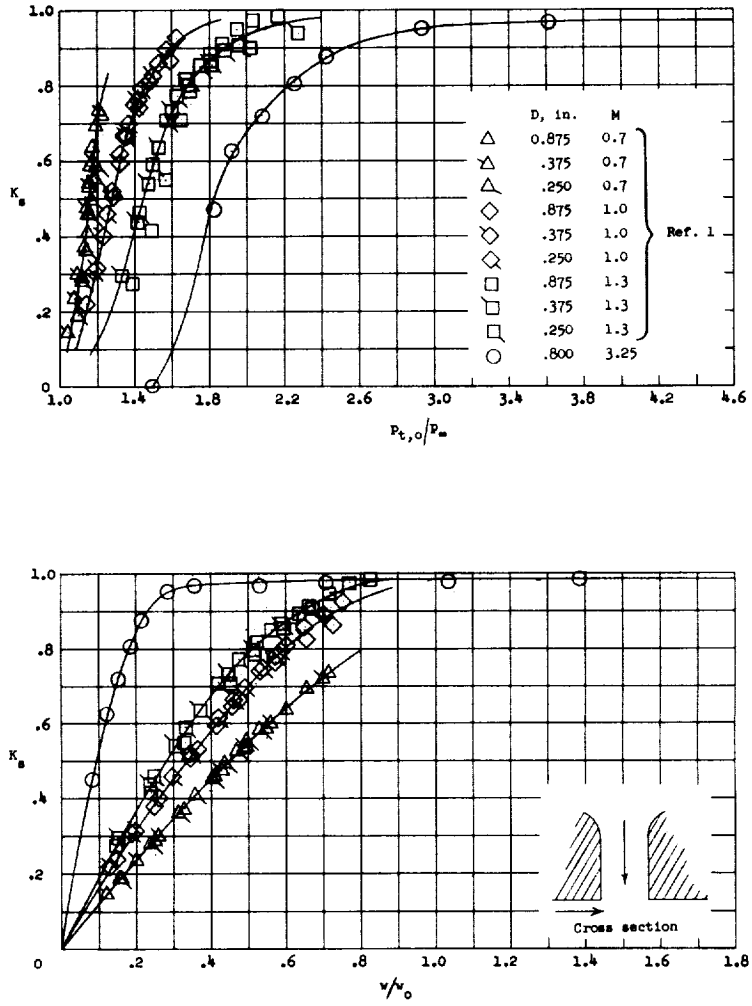

(b) Circular ducted outlet 10. $\beta = 90^\circ$.

Figure 8.- Continued.

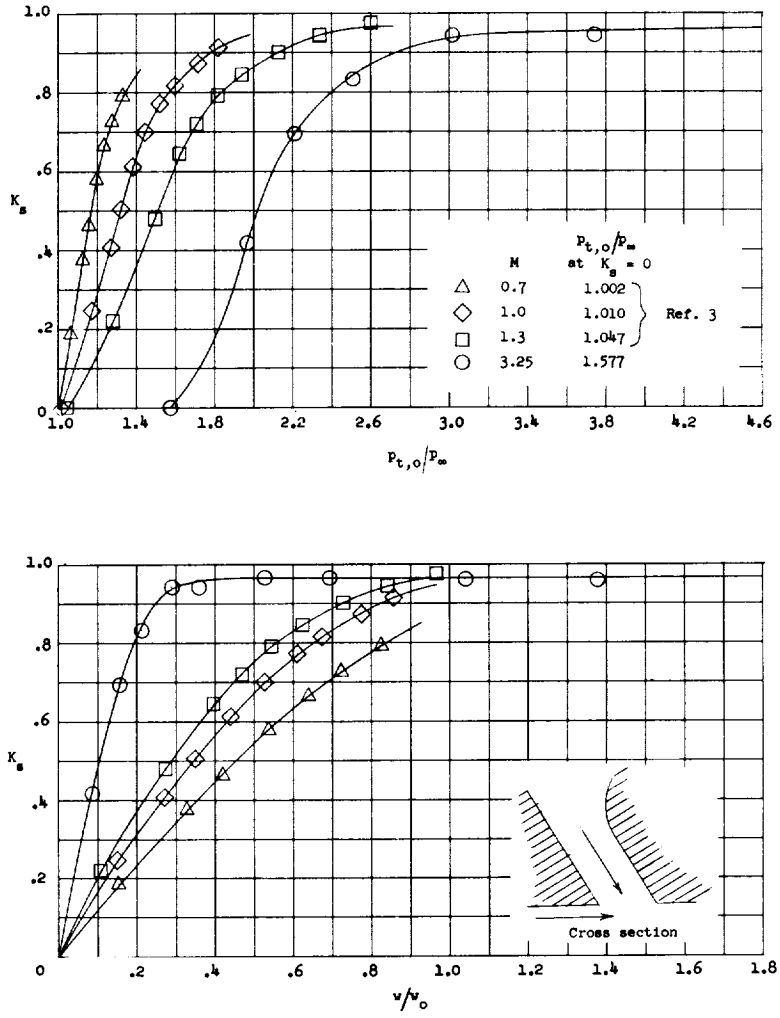

(c) Square ducted outlet 12. $\beta = 60^\circ$.

Figure 8.- Continued.

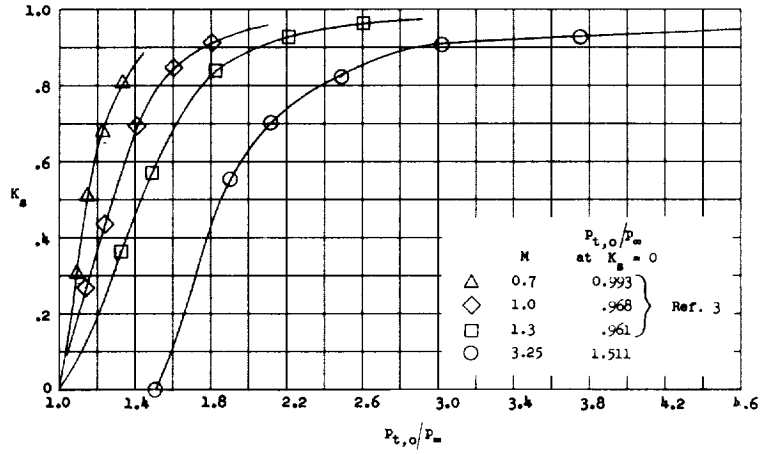

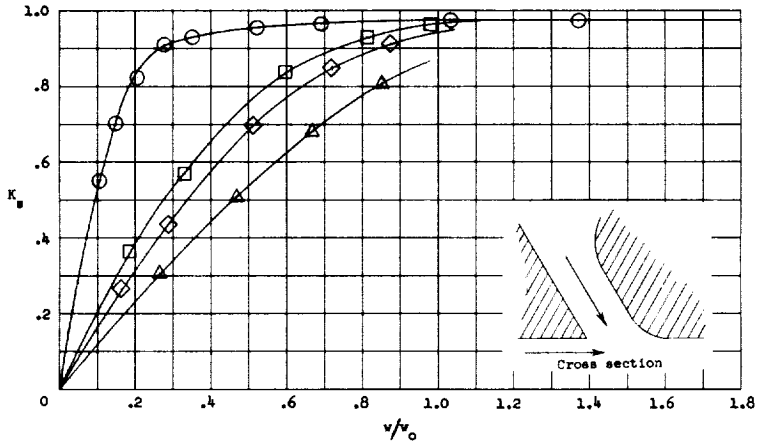

(d) Square ducted outlet 13. $\beta = 60^\circ$; 0.5-in. radius on downstream side.

Figure 8.- Continued.

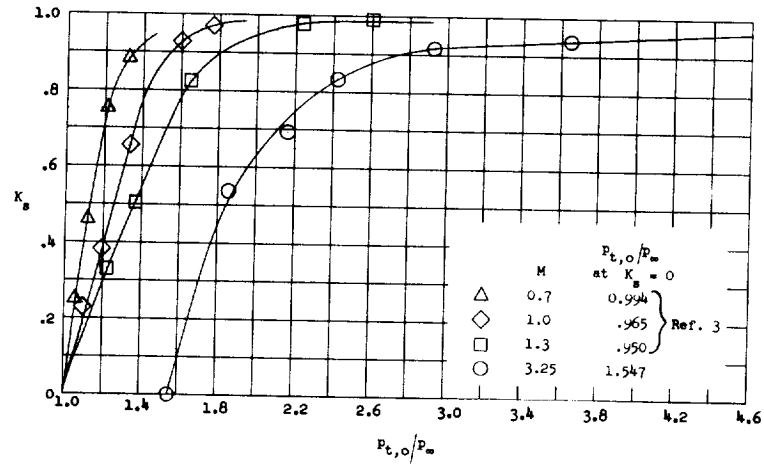

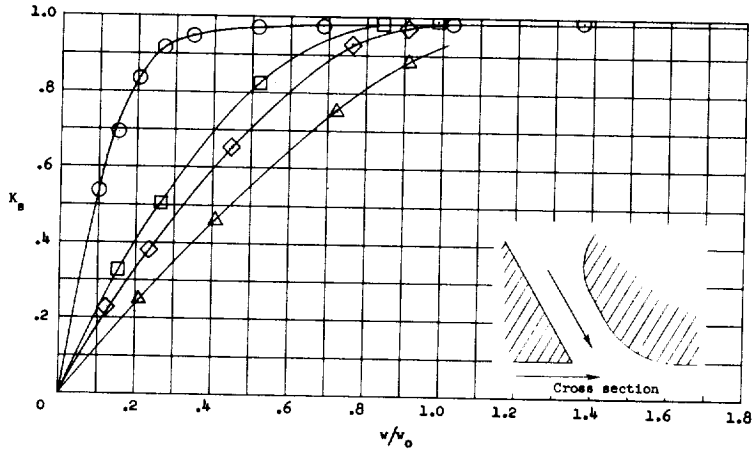

(e) Square ducted outlet 14. $\beta = 60^\circ$; 1-in. radius on downstream side.

Figure 8.- Continued.

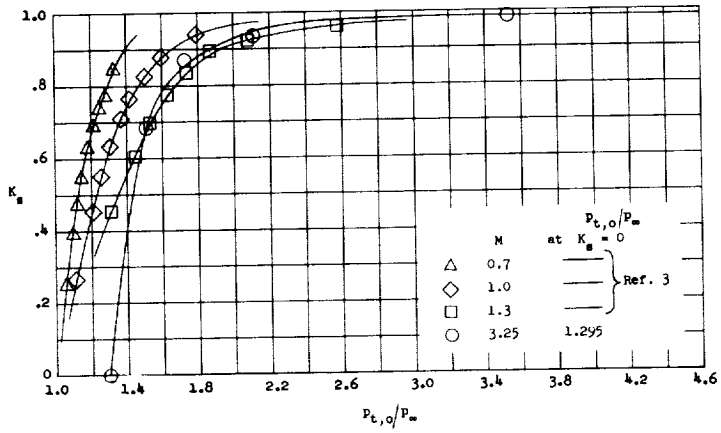

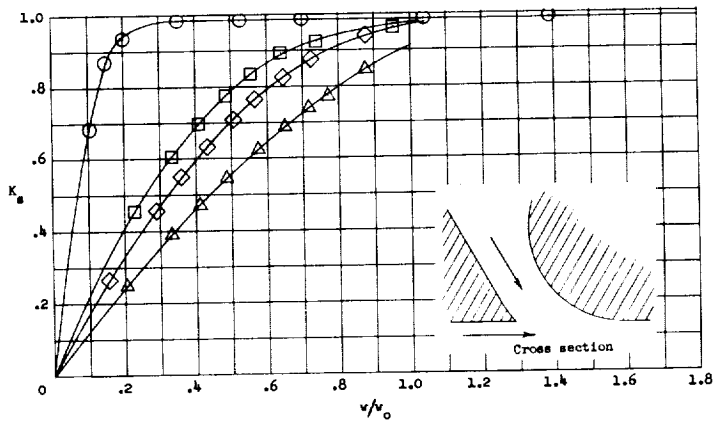

(f) Square ducted outlet 16. $\beta = 50.5^{\circ}$; curved radius on upstream and downstream sides.

Figure 8.- Continued.

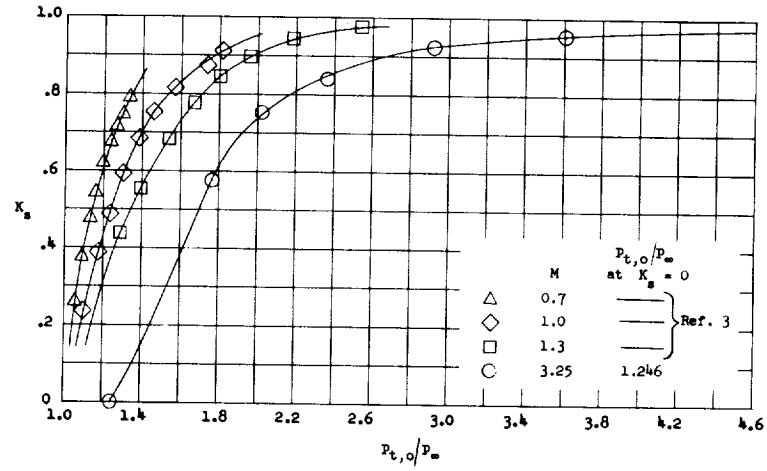

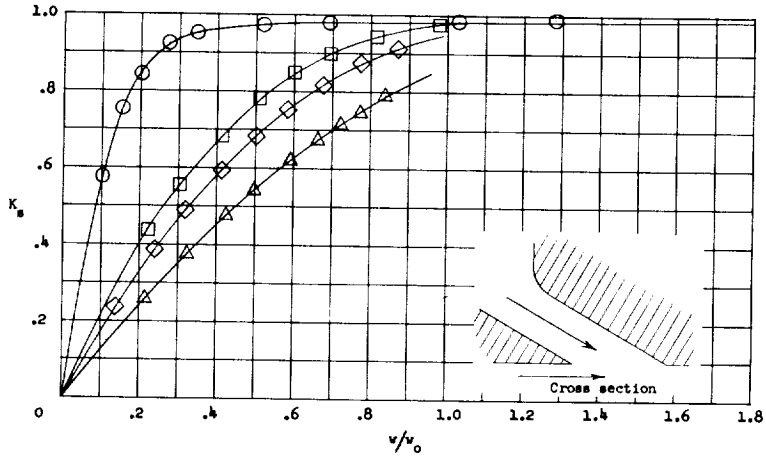

(g) Square ducted outlet 15. $\beta = 30^\circ$.

Figure 8.- Continued.

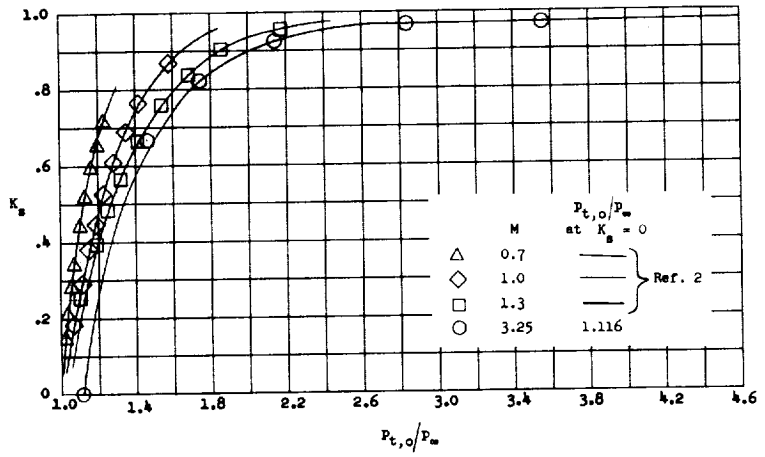

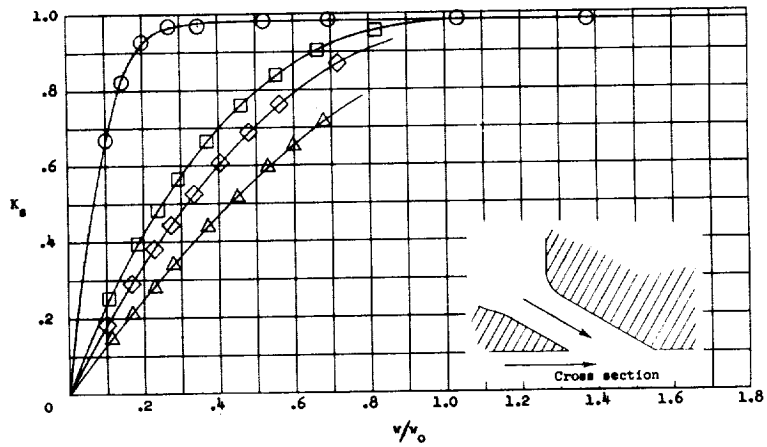

(h) Circular ducted outlet 11. $\beta = 30^\circ$.

Figure 8.- Concluded.

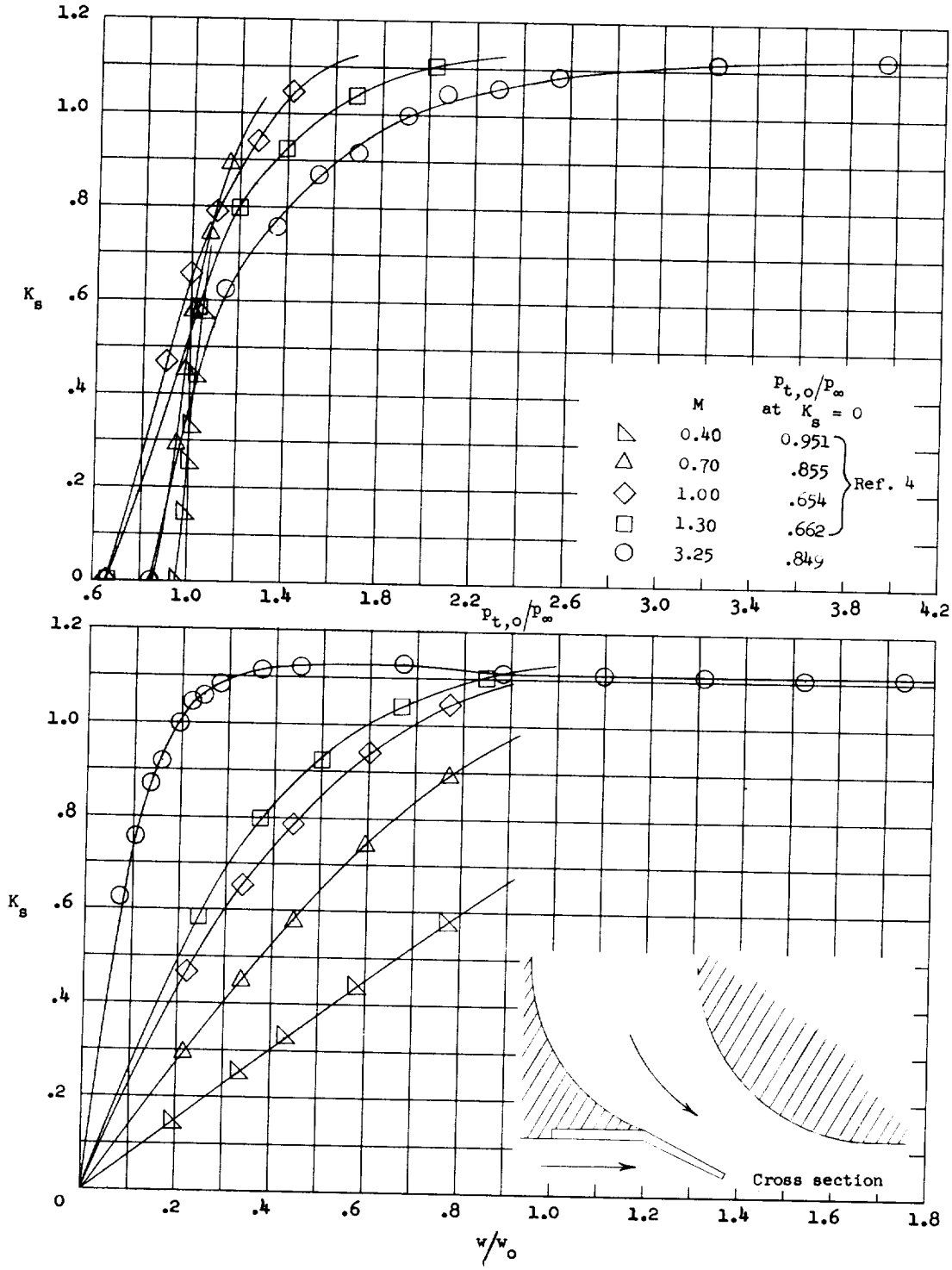

Figure 9.- Discharge characteristics for flapped outlet 17. $\delta_f = 25°21'$.

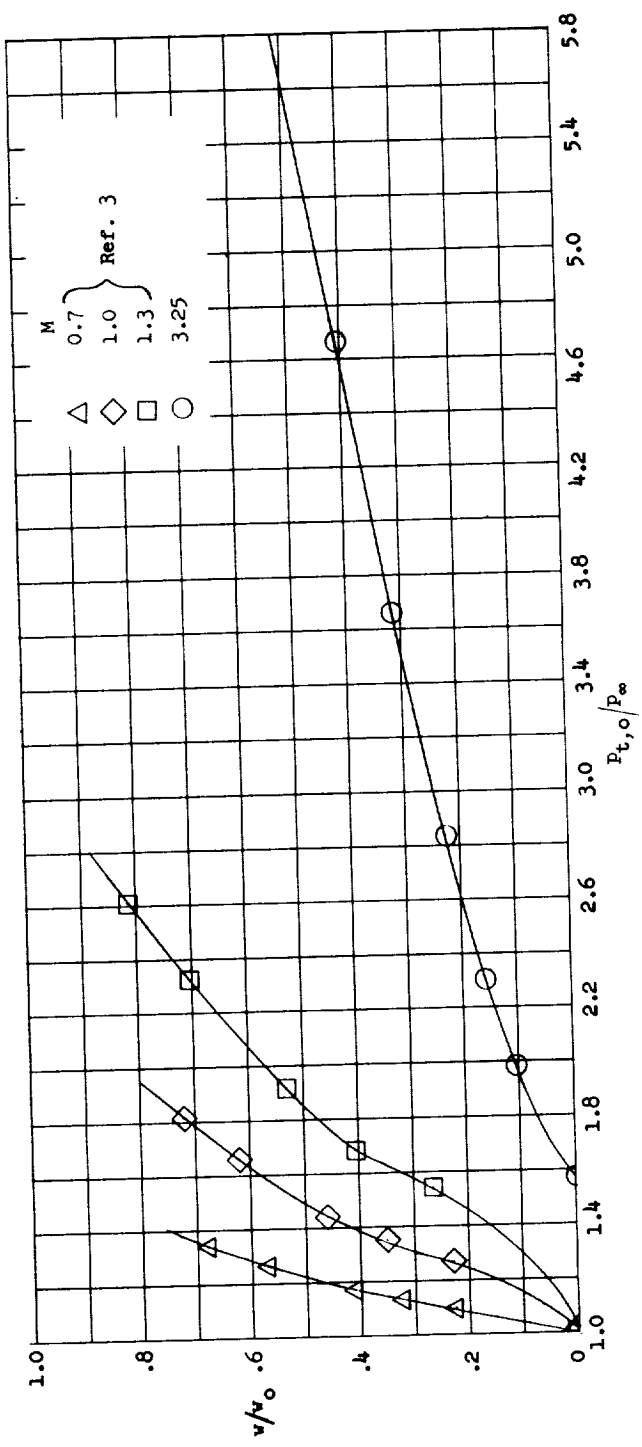

Figure 10.- Variation of discharge-flow ratio with pressure ratio for thin-plate outlets.
A = 1.0.

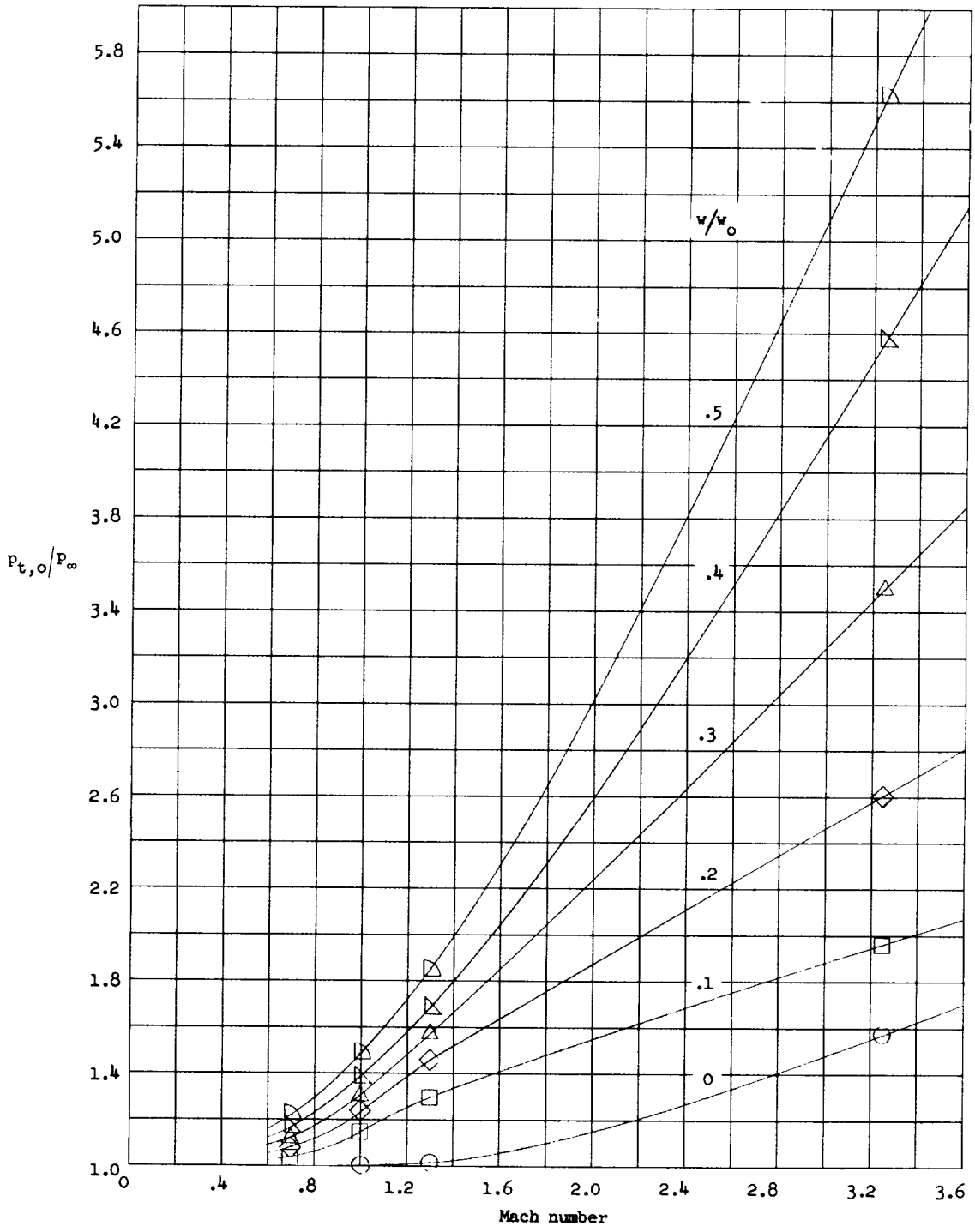

Figure 11.- Cross plot of figure 10 showing variation of pressure ratio with Mach number for constant values of discharge-flow ratio.

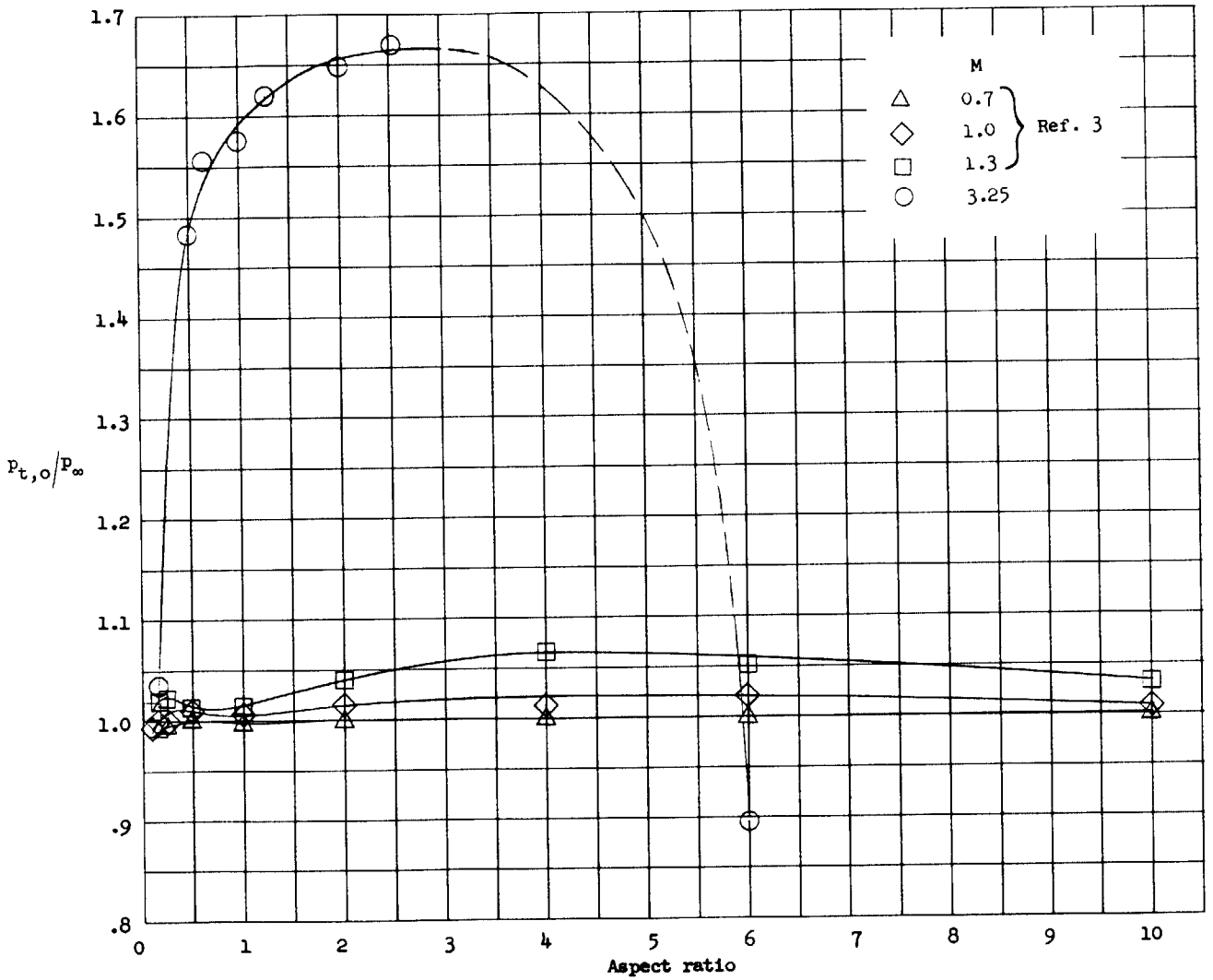

Figure 12.- Variation of no-flow-pressure ratio with aspect ratio for thin-plate outlets.

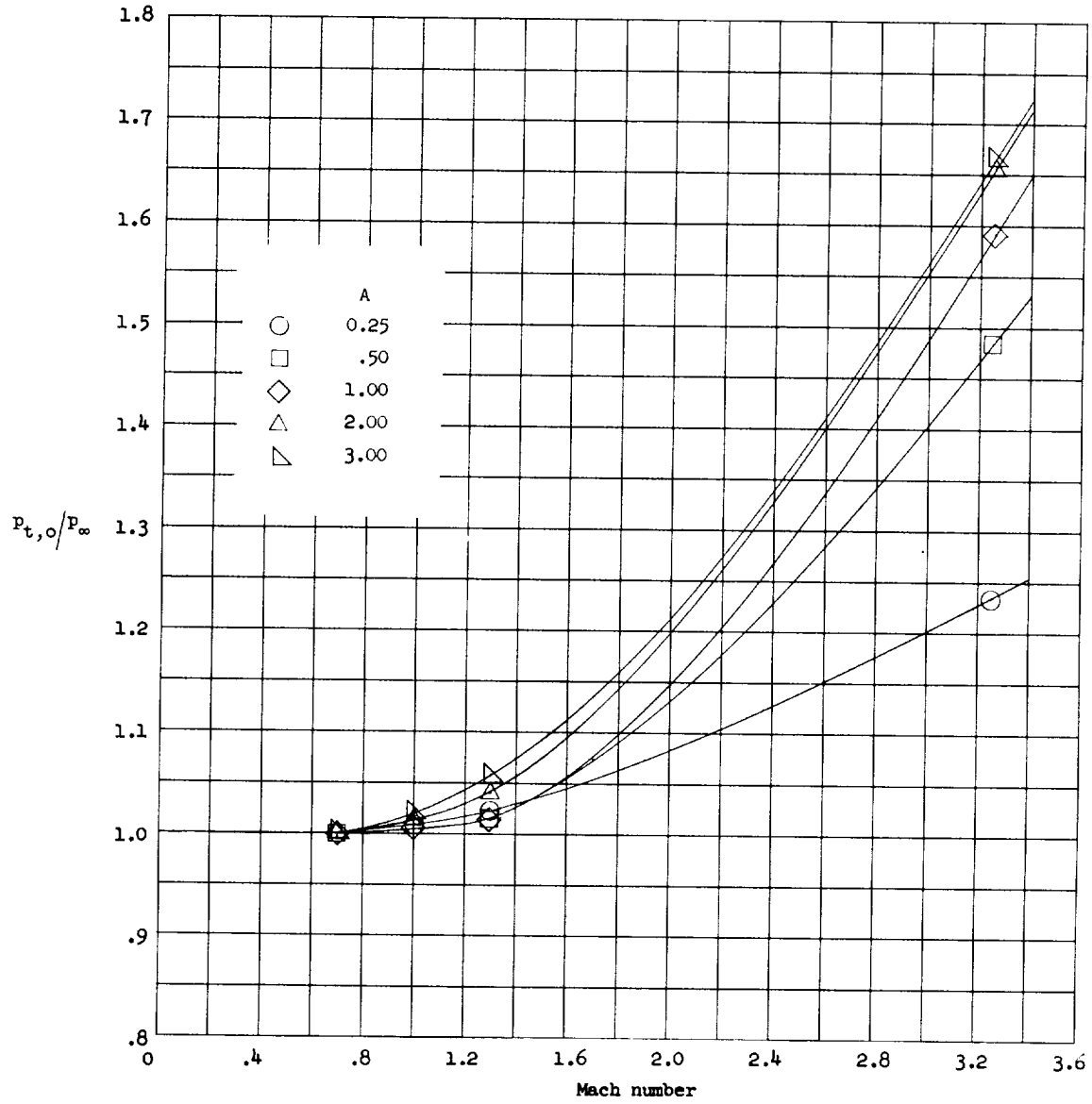

Figure 13.- No-flow pressure ratio plotted against Mach number at varying aspect ratios for thin-plate outlets. Data for Mach numbers of 0.7, 1.0, and 1.3 are cross plotted from reference 3.

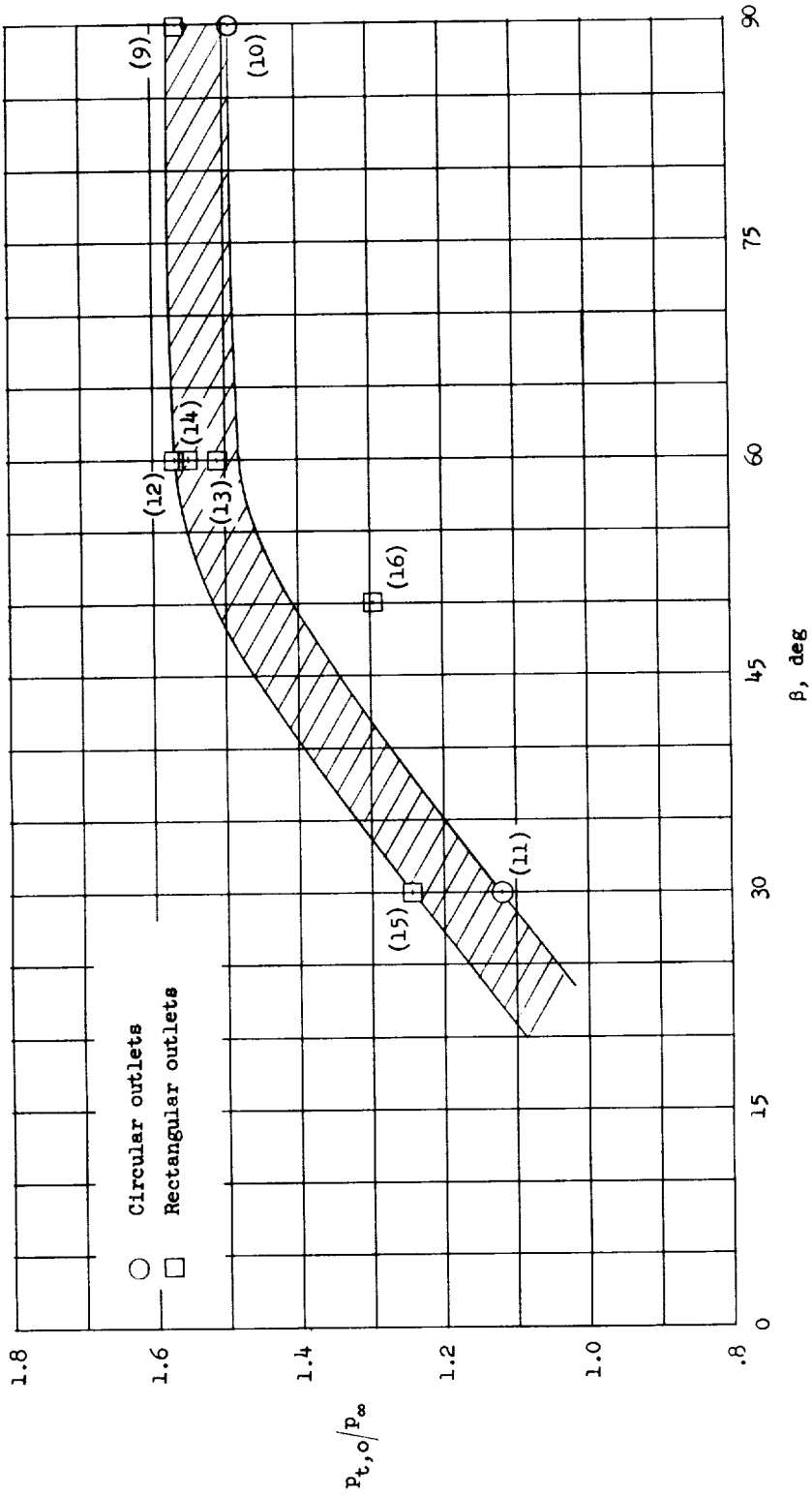

Figure 14.- Variation of no-flow pressure ratio with angle of inclination for ducted outlets. (Numbers in parentheses refer to outlets.)

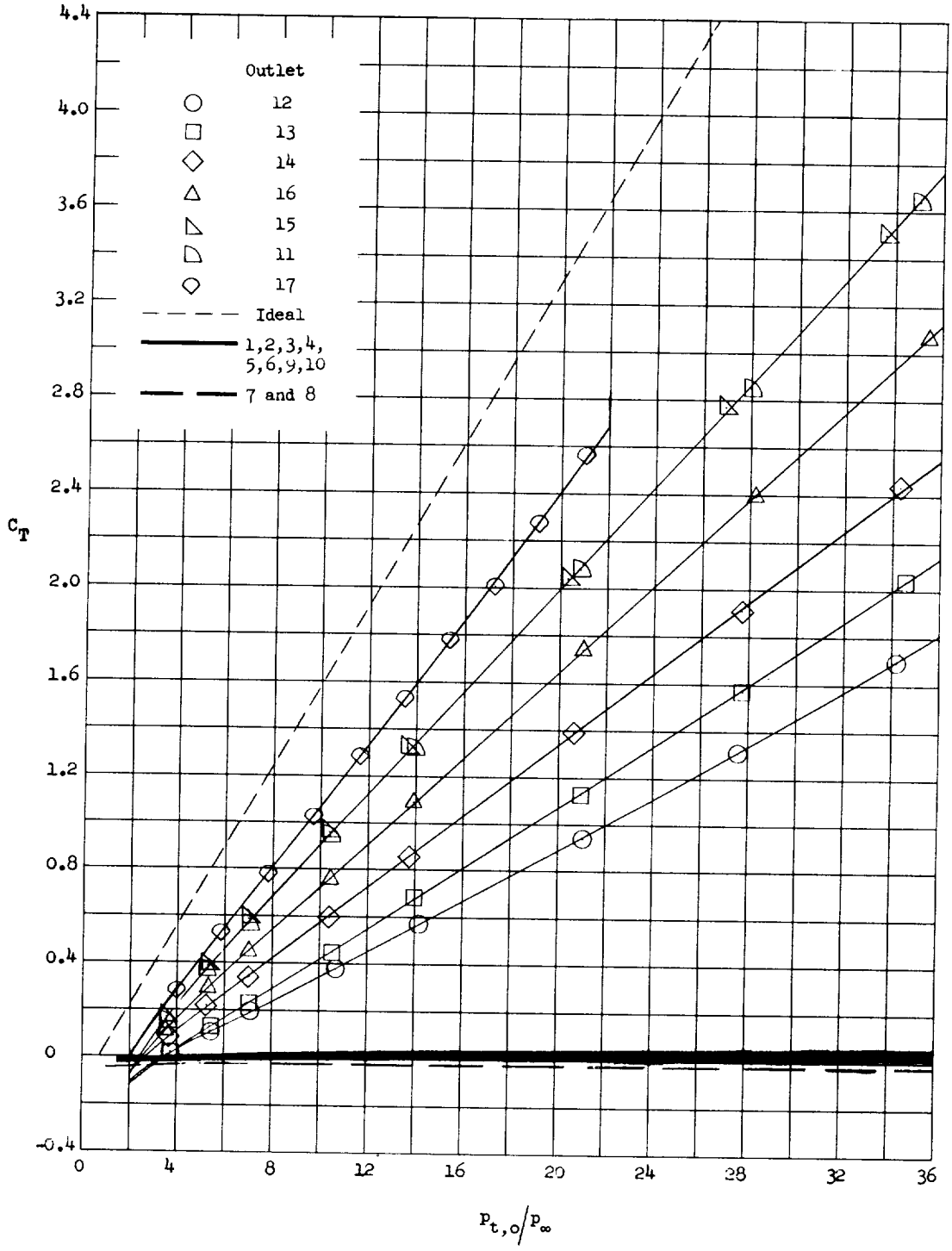

Figure 15.- Variation of thrust coefficient with pressure ratio for all outlets.

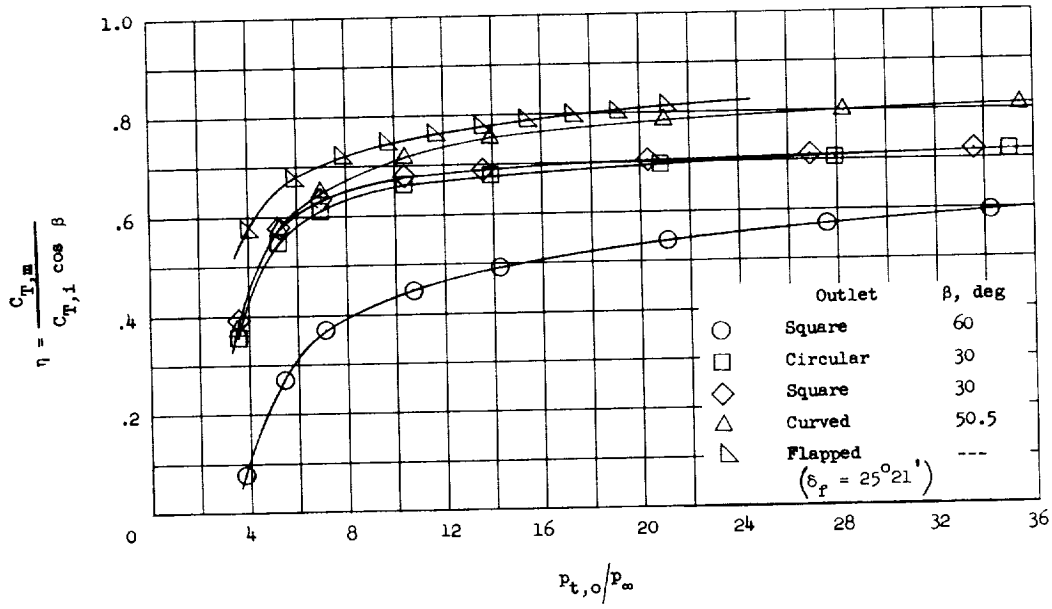

(a) Effect of variation of outlet shape and angle of inclination.

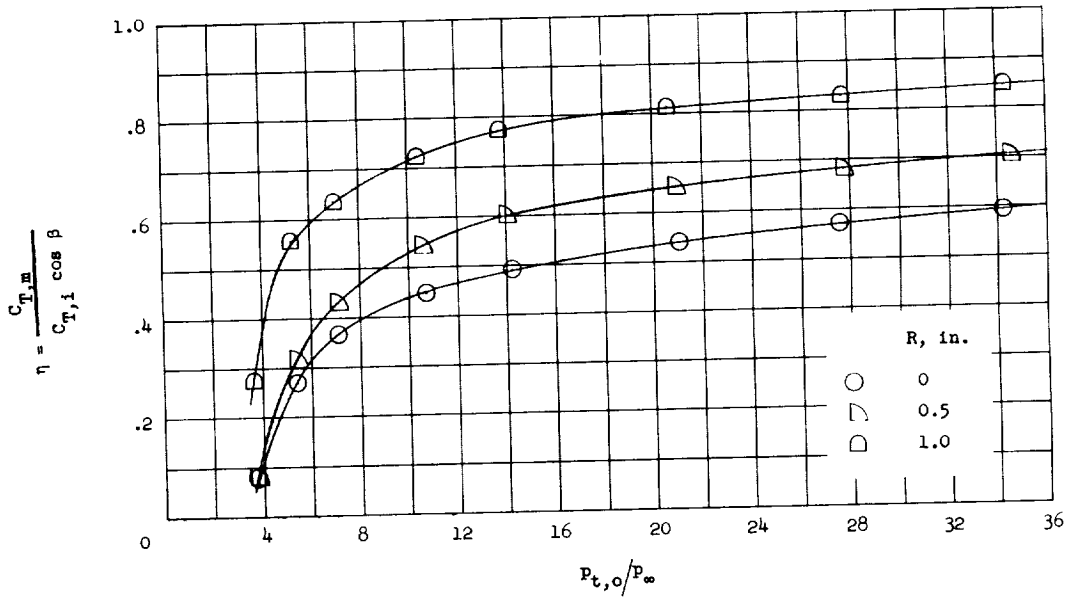

(b) Effect of varying radius of curvature on downstream end of square ducted outlet. $\beta = 60^\circ$.

Figure 16.- Thrust efficiency plotted against pressure ratio for ducted outlets.

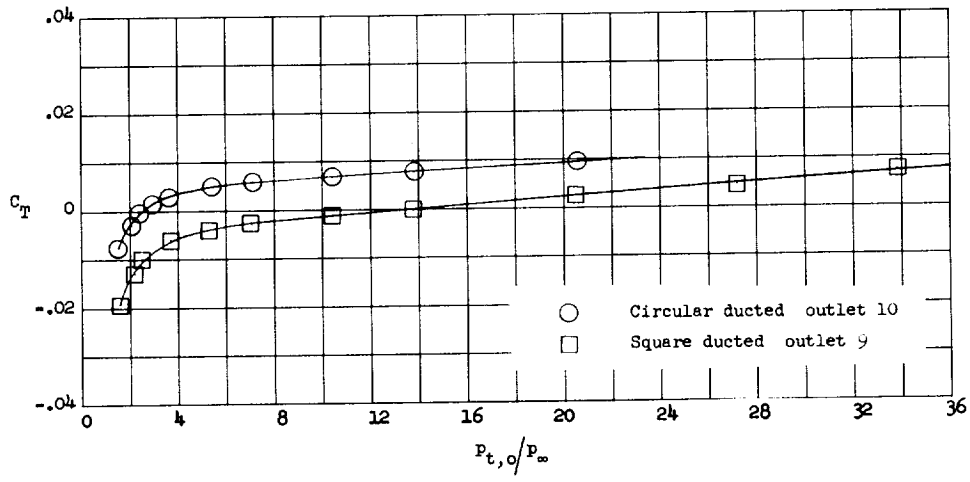

(a) Expanded scale of thrust coefficient for perpendicularly ducted outlets.

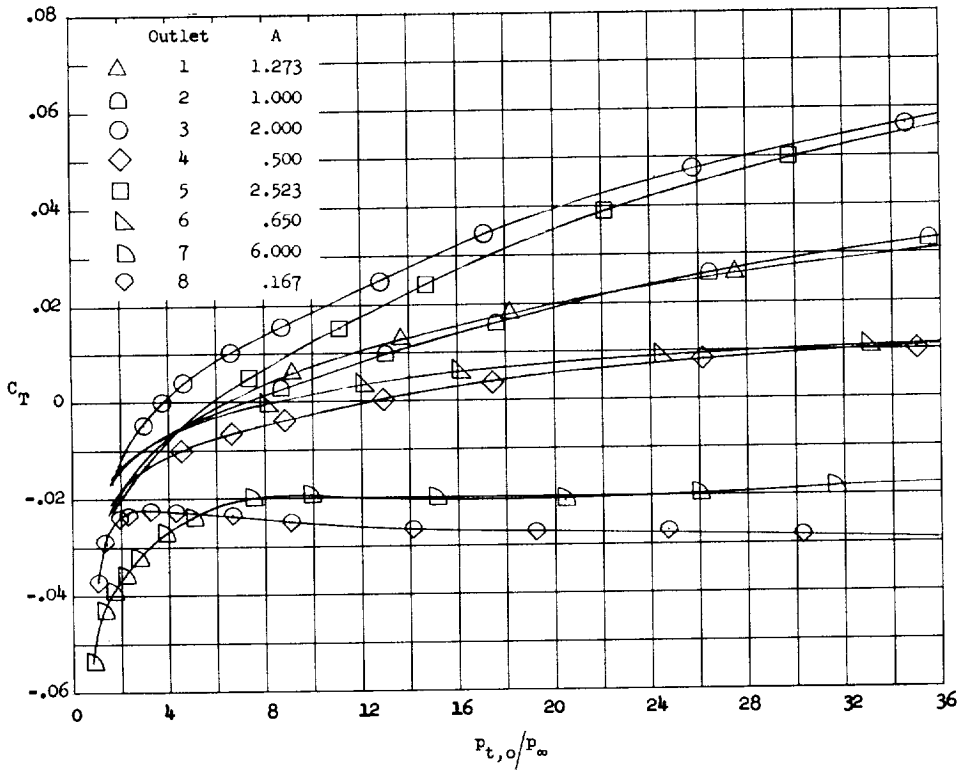

(b) Expanded scale of thrust coefficient for all thin-plate outlets.

Figure 17.- Variation of thrust coefficient with outlet pressure ratio.

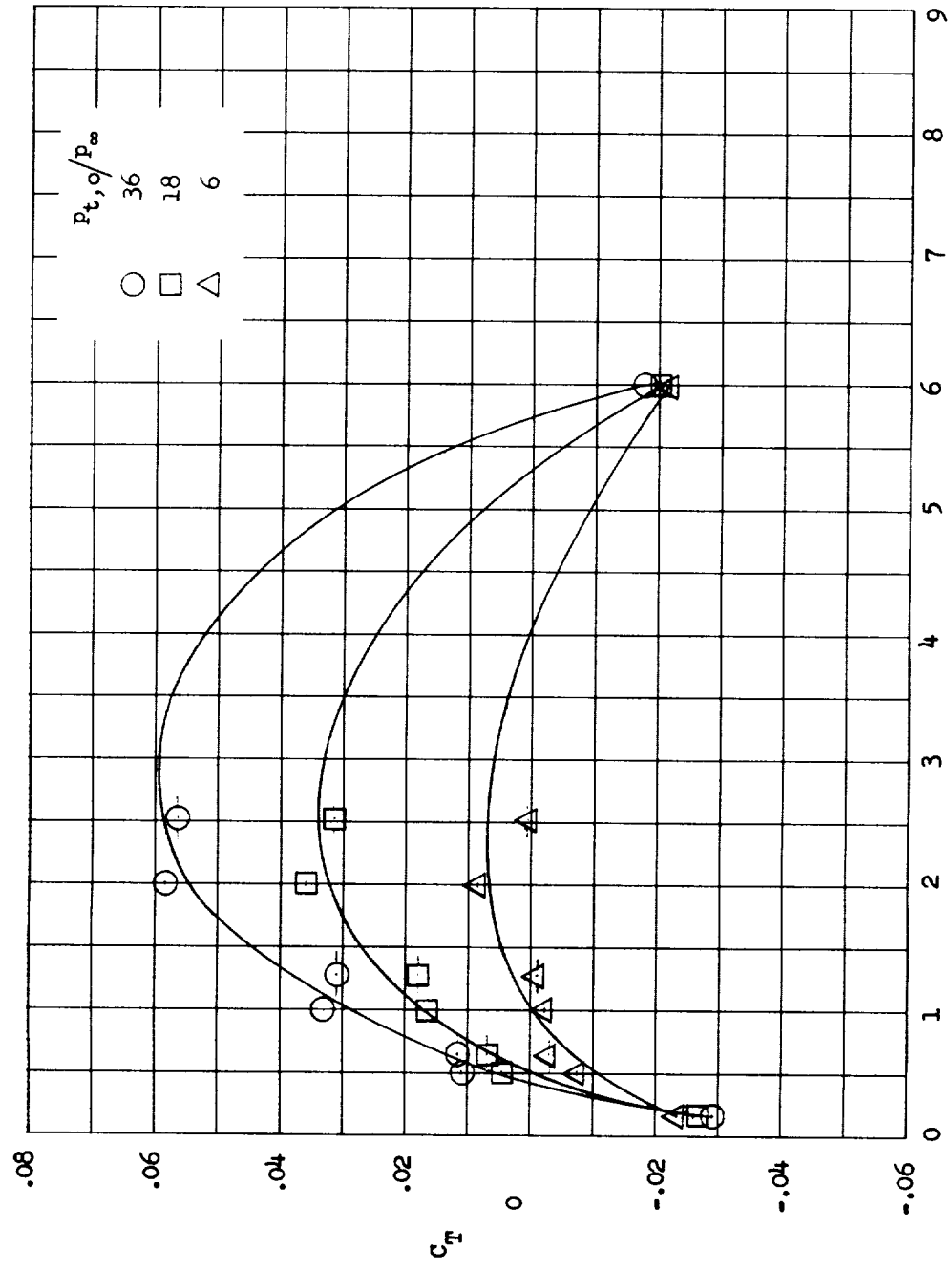

Figure 18.- Variation of thrust coefficient with aspect ratio for thin-plate outlets at constant values of pressure ratio. (Ticks on symbols indicate circular or elliptical outlet.)

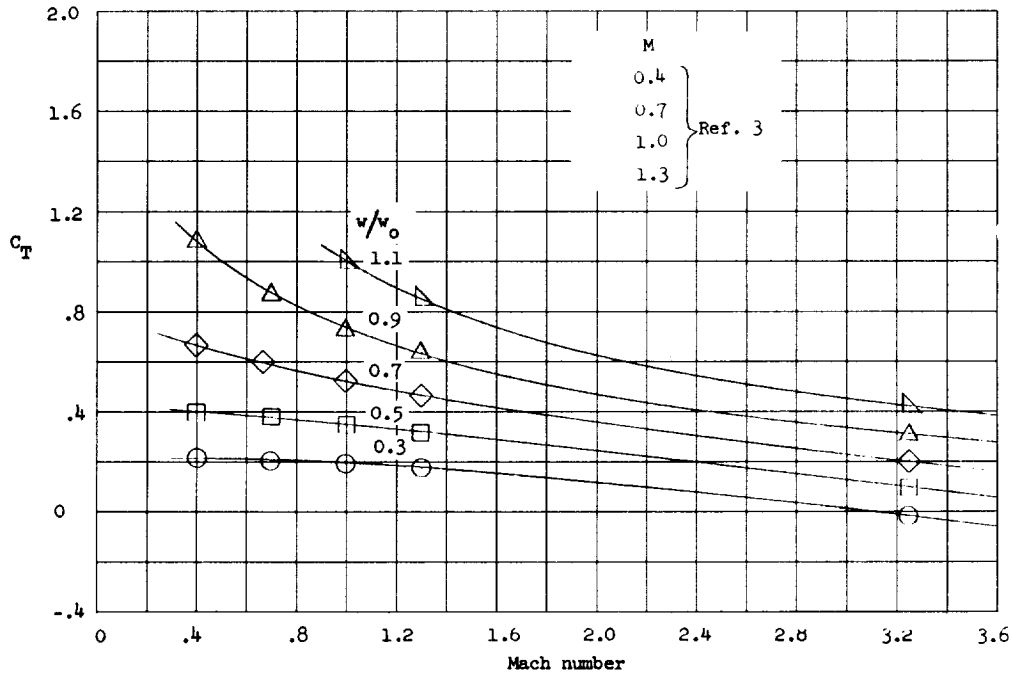

(a) Square ducted outlet. $\beta = 60^{\circ}$.

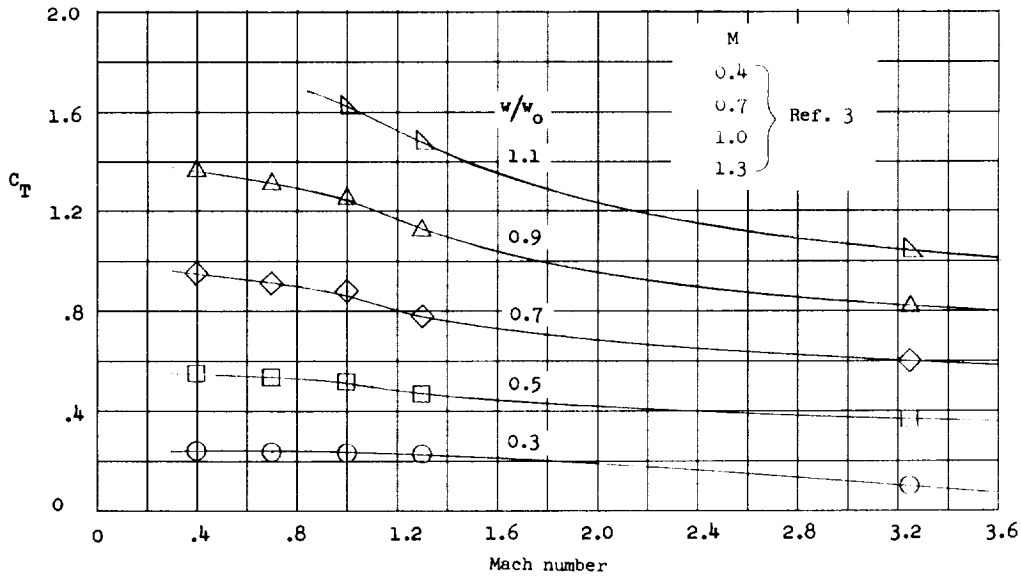

(b) Circular ducted outlet. $\beta = 30^{\circ}$.

Figure 19.- Variation of thrust coefficient with Mach number.

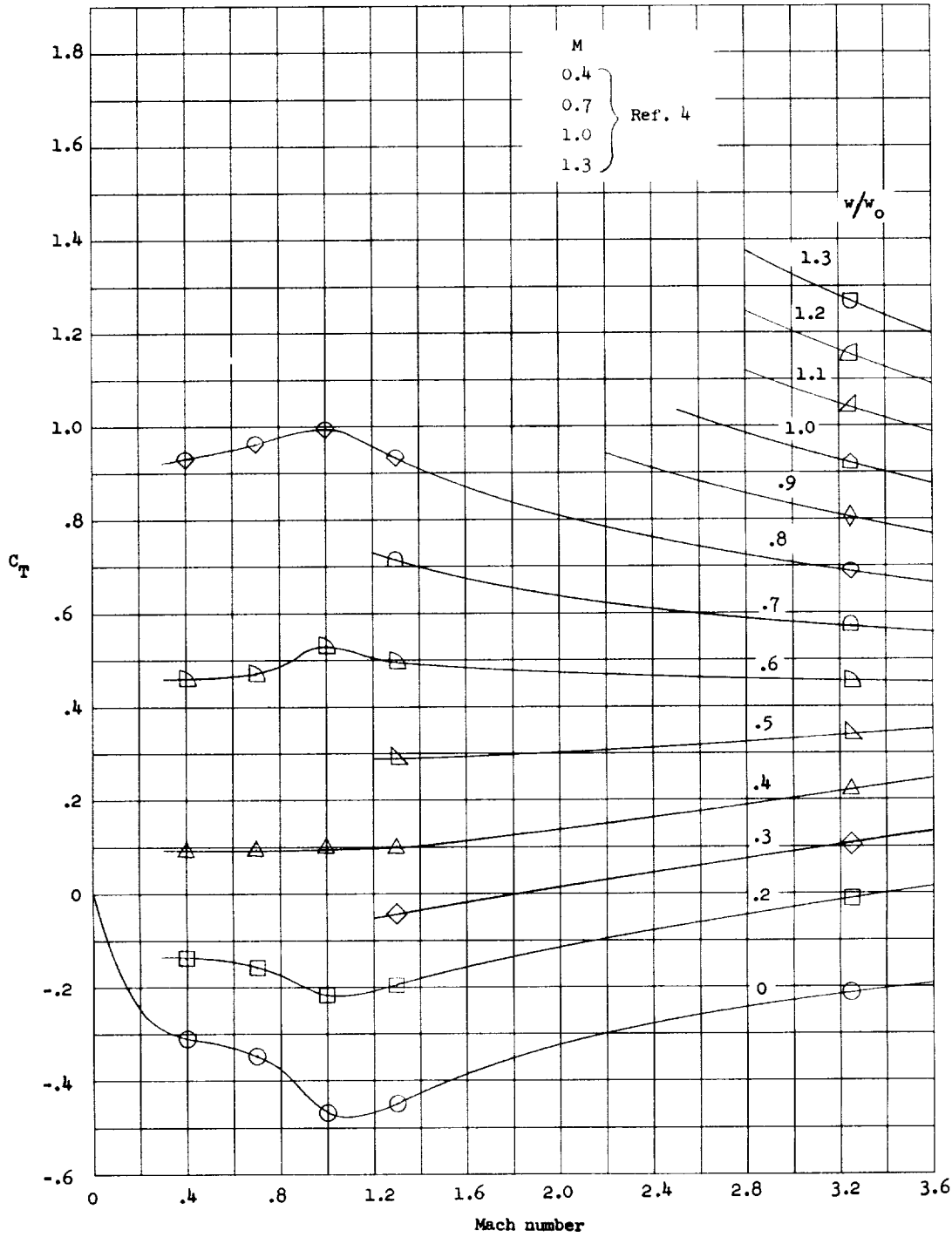

Figure 20.- Variation of thrust coefficient with Mach number at constant values of discharge-flow ratio for flapped outlet. $\delta_f = 25°21'$.

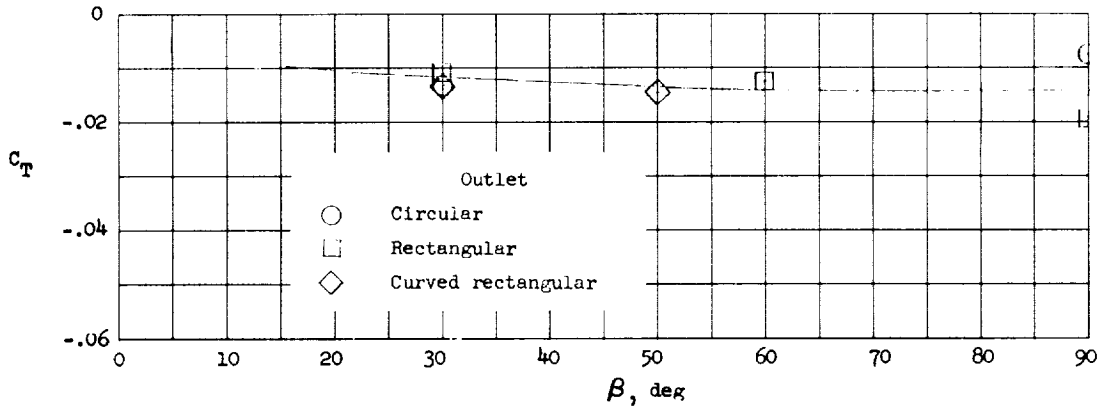

(a) Ducted outlets.

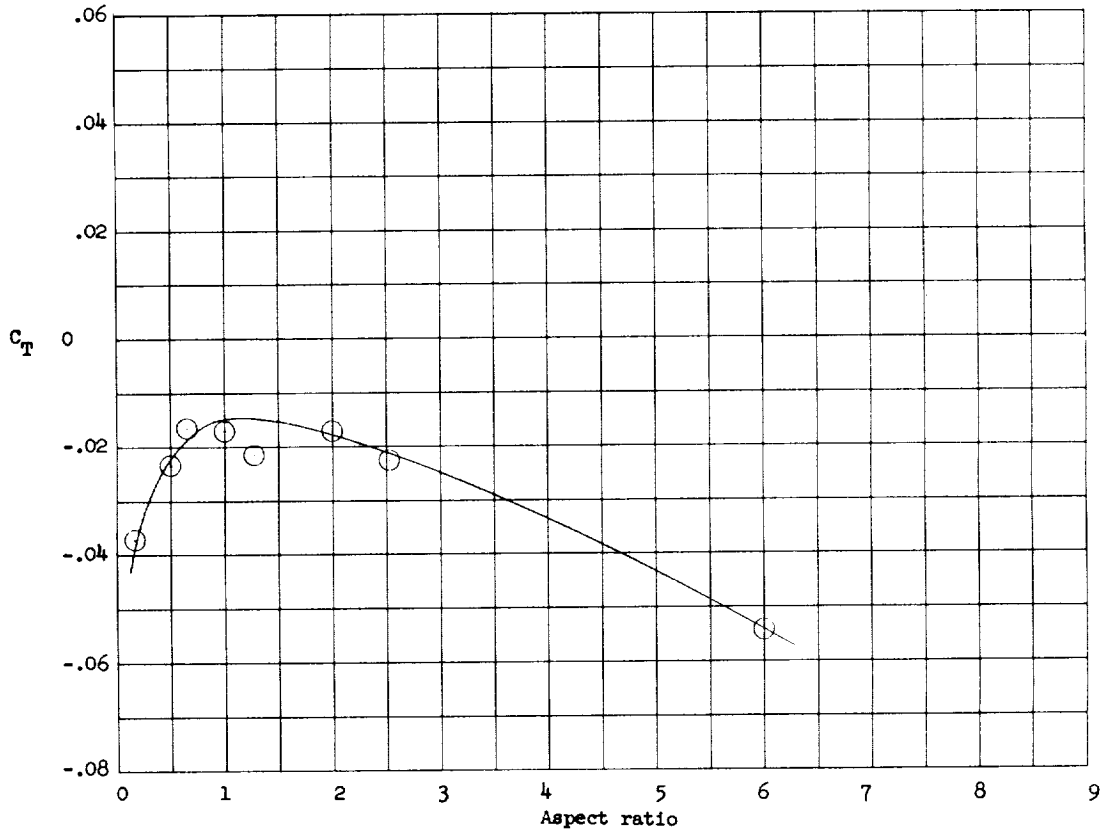

(b) Thin-plate outlets.

Figure 21.- Thrust coefficient at no flow for ducted and thin-plate outlets.